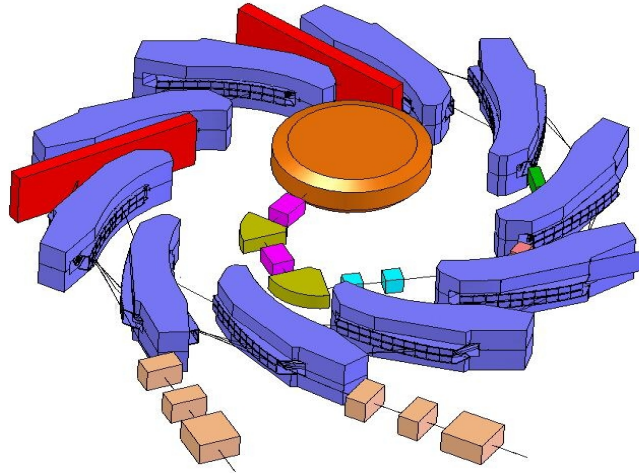


# ***RACCAM***

F. Méot  
CEA & IN2P3  
LPSC, Grenoble



*An ANR contract, Feb. 2006 – Feb. 2009*

- A status, including :
- Magnet prototyping
  - Magnetic measurements

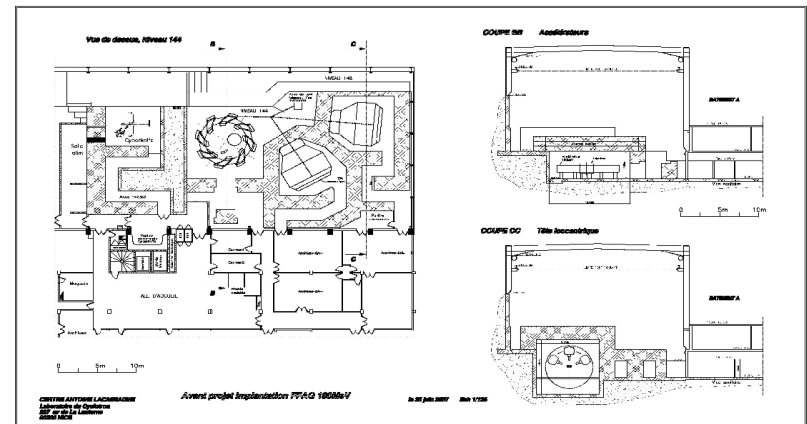
# Motivations for a project of a protontherapy FFAG

(i) Hadrontherapy is considered to be more effective for cancer treatment comparing to photons

(ii) FFAGs appear to have various advantages in medical applications:

- Potential for variable energy operation ( → no need of degrader, ESS)
- High dose delivery, potentially  $\gg$  Gy/min (←high rep rate, potentially 100s Hz)
- Potential for reasonably compact size (if needed...) and low cost
- Flexibility : synchrotron-like manipulation of beams  
(injection, extraction, multi-particle)
- Stable and easy operation (← fixed magnetic field)
- Potential for multiple extraction ports
- Natural scanning method : bunch-to-voxel

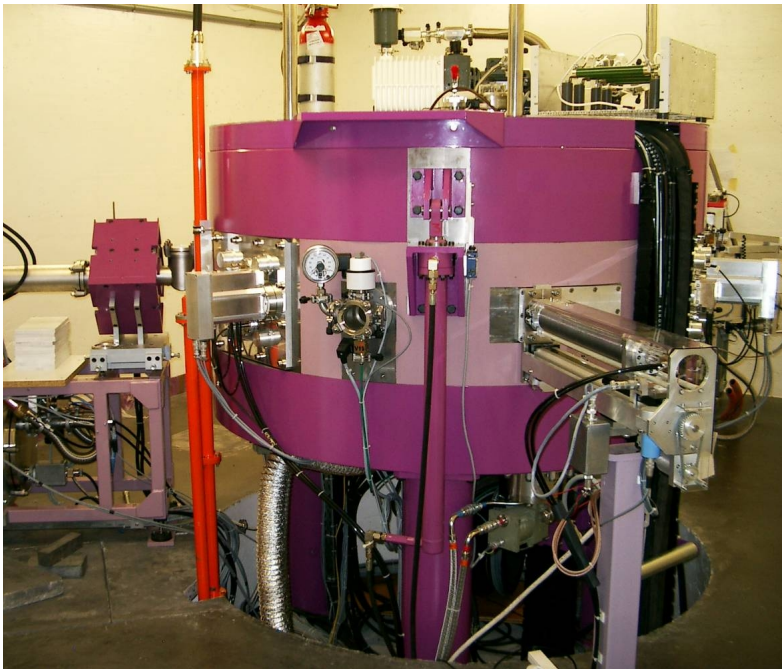
(iii) Possible implementation of a demonstration machine at the Nice anti-cancer clinic (MEDICYC)



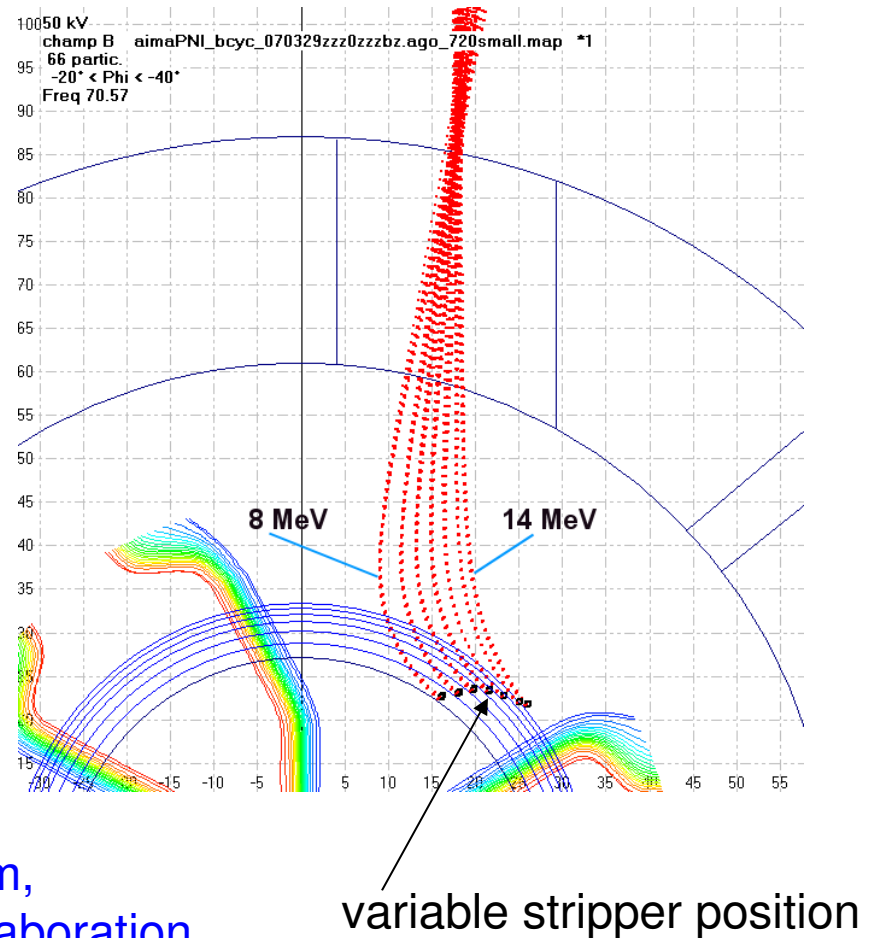
# Principle of RACCAM injector : Tunable energy proton beam

## Involves using a H<sup>-</sup> cyclotron injector

AIMA H<sup>-</sup> cyclotron – our injector for FFAG

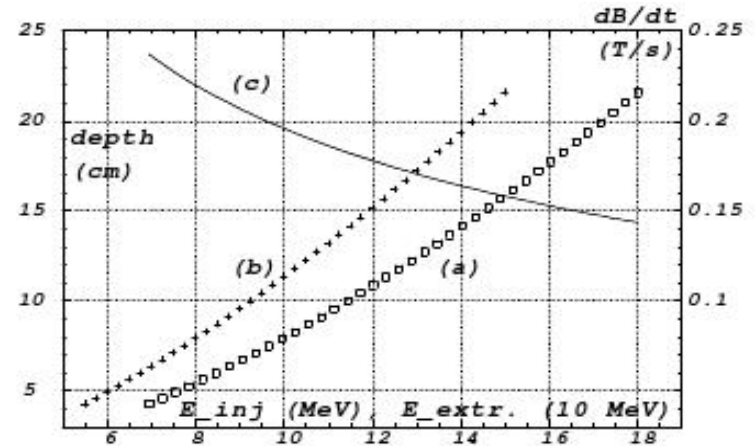
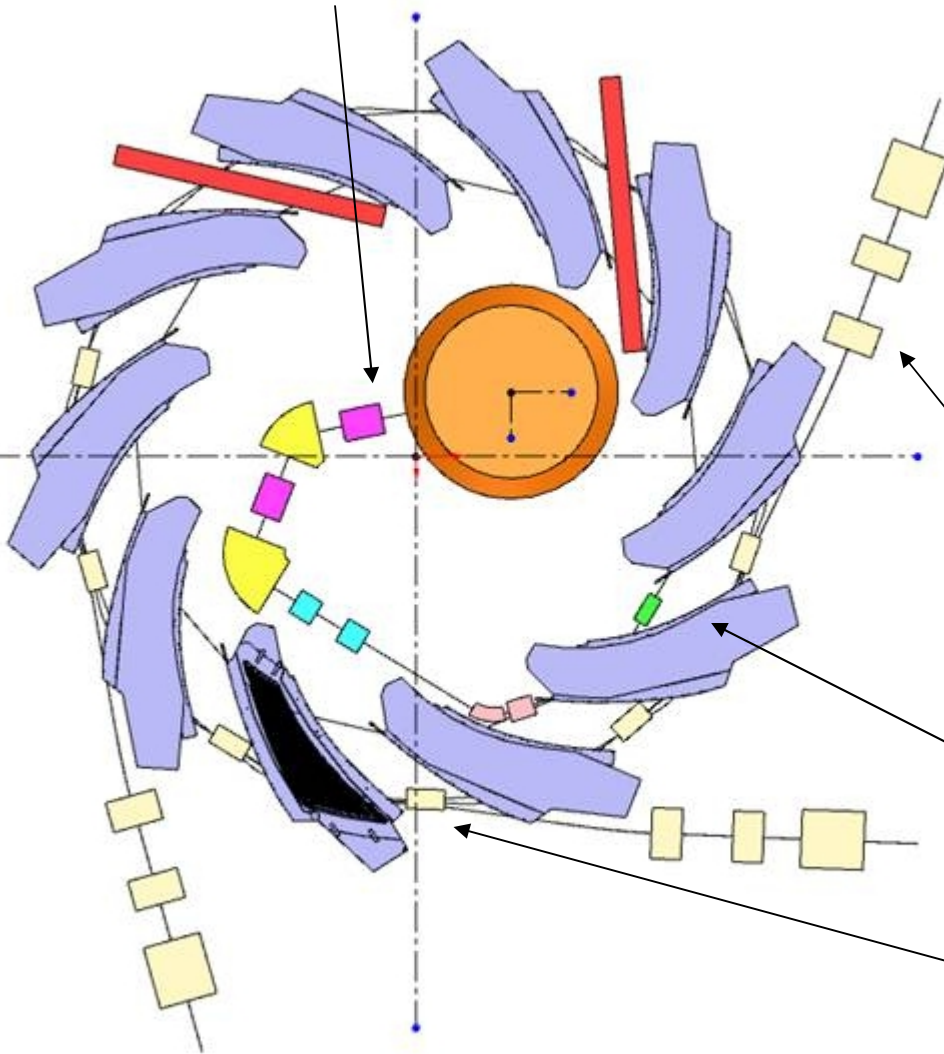


Studies made by AIMA-Development team, MEDICYC, Nice, as part of RACCAM collaboration



# Principles of energy variation :

Variable extraction energy from  
H<sup>-</sup> cyclotron injector



- (a) : Bragg pic depth as a function of FFAG extraction energy
- (b) : correlated cyclotron energy with 250kV steps
- (c) : dB/dt

allows variable extraction energy from FFAG

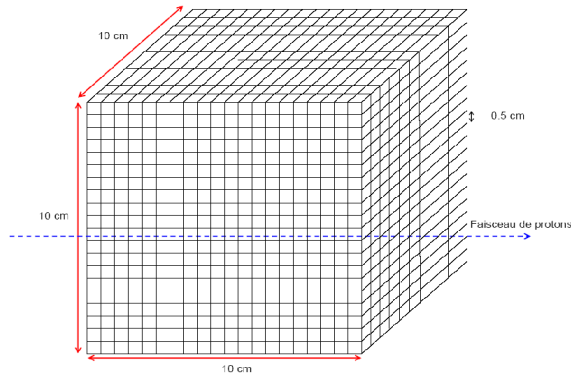
by varying FFAG rigidity and / or by extraction kick synchronised on turn #

# Beam delivery hypothesis

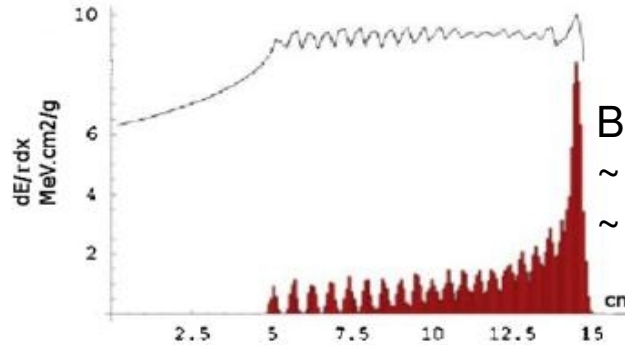
## (ii) Spread out Bragg pic (SOBP) :

### (i) Reference volume :

- 1 liter cube, 10x10x10cm<sup>3</sup>
- Voxel size : 5x5x5 mm<sup>3</sup>



$$\left| -\frac{dE}{dx} \right| = 2\pi N_a r_e^2 m_0 c^2 \rho \frac{Z}{A} \frac{z^2}{\beta^2} \left[ \ln \left( \frac{2m_0 \gamma^2 v^2 W_{\max}}{I^2} \right) - 2\beta^2 - \delta - 2\frac{C_s}{Z} \right]$$



Basic results :

- ~ 7 10<sup>11</sup> proton/Gy in a liter
- ~ only weak dependence on E

### (iii) Bunch filling for bunch-to-pixel scanning :

- **400 pixels/slice**, about 20% of the dose in the distal layer, yields a maximum 5Gy x 7.10<sup>11</sup> p/Gy x 20% / 400pixel ~ **2x10<sup>9</sup> p/pixel in the distal layer**
- Cyclotron produces 1.5x10<sup>7</sup> ppb, hence need ~ **130 cyclotron bunches**
- Cyclotron RF 70MHz (h=3) and FFAG 3MHz @ injection, i.e. 70MHz/3MHz\*h3 = **70 cyclotron bunches in one FFAG turn.**

Hence, for distal pixels,

either (i) 5-turn injection at 50% efficiency

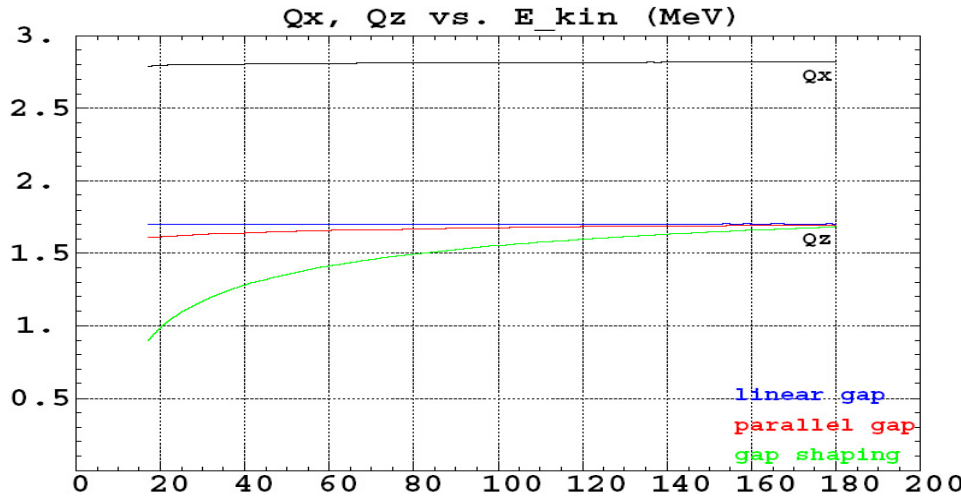
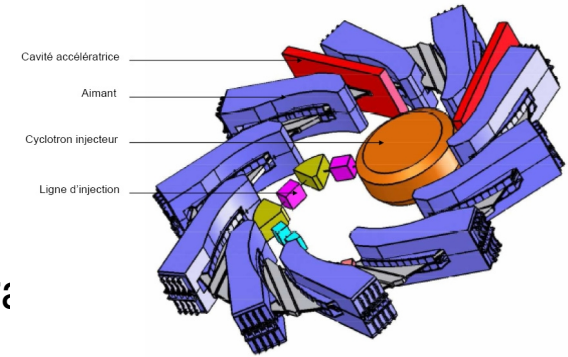
or (ii) single-turn injection and a minimum of 4 paintings

(iv) Repetition rate needed : 20x20x20 pixels in a minute, hence, ~130Hz

# Scaling magnet – a delicate problem to deal with :

## Vertical focusing:

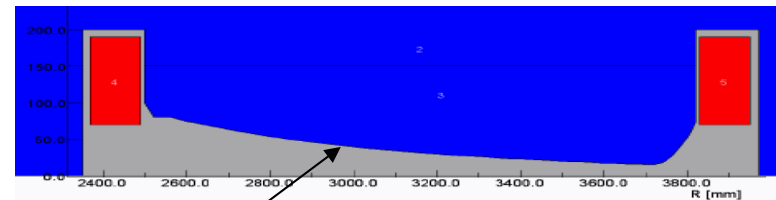
- strongly influenced by fringe fields
- difficult to obtain constant  $Q_v$
- especially when planning varying field for variable energy
- yet, the theory is well known, confirmed by stepwise ray-tr



$$M_z = \begin{pmatrix} 1 & 0 & 0 \\ -\frac{\tan(\delta - \psi)}{\rho} & 1 & 0 \\ 0 & 0 & 1 \end{pmatrix}$$

$$\psi = I_1 \frac{\lambda}{\rho} \frac{1 + \sin^2(\delta)}{\cos(\delta)} \quad r = \rho x \frac{\sin\left(\frac{\pi}{N}\right)}{\sin\left(p_f \frac{\pi}{N}\right)}$$

$$I_1 = \int_{-\infty}^{\infty} \frac{B_z(s) [B_{z0} - B_z(s)]}{\lambda B_{z0}^2} ds$$



Scaling, requires

$$\psi = Cst \rightarrow \lambda \sim r$$

Magnetic field  $B \sim r^k$

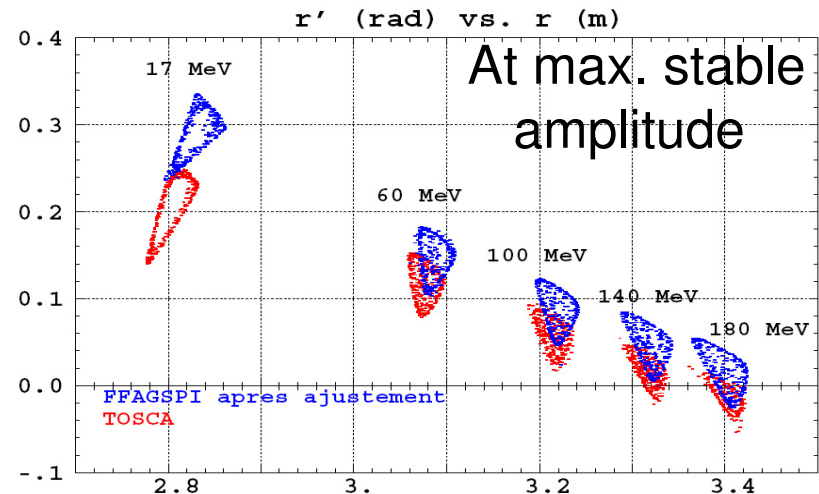
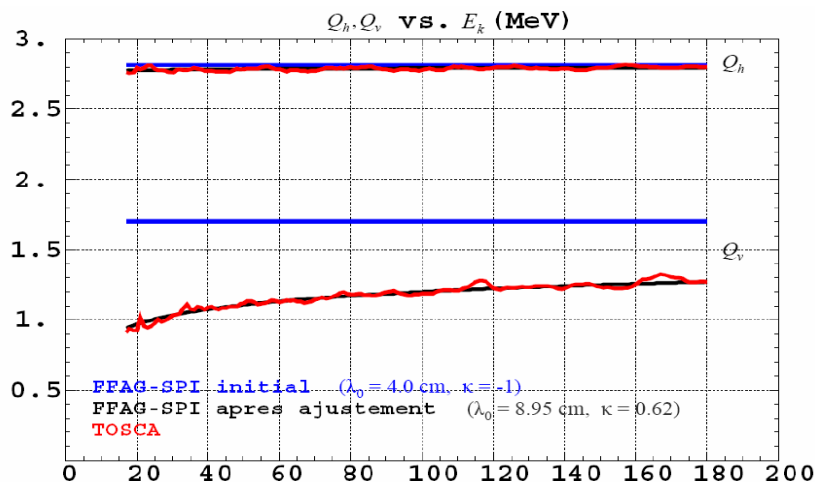
requires  $\lambda \sim \text{gap} \sim 1/r^k$

**Conflict!**

## We have used 2 different tools to simulate the field :

- Either TOSCA that generates field maps,  
yet too slow for beam dynamics optimization method
  - Or “FFAG-SPI/Zgoubi” based on analytical model of the spiral field,  
very fast
- Magnet prototype design and ring design have been a permanent feedback between the two methods :
    - TOSCA field maps when precision is needed
    - “FFAG-SPI” when optimization speed is needed
  - A sample of the agreement between both :

→ main knob for good match : fringe field extent,  $\lambda$



# We end up with a set of optimized parameters of the RACCAM 10 cell ring and magnet :

Extraction energy, variable (MEDiCYC specs.)

Injection energy

Momentum ratio

Number of cells

Packing factor

Field index, k

Spiral angle

$Q_h / Q_v$

Radius on extraction/injection orbit : dR

Drift length, extraction/injection orbit

Frev, 15->180 MeV

Frev, 5.5->70 MeV

70 – 180 MeV

5.5 – 17 MeV

3,62

10

0,34

5

53.7 deg.

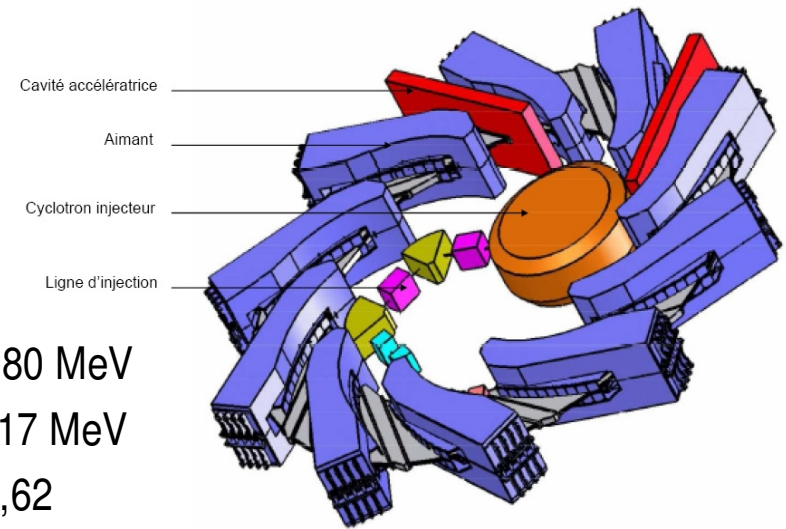
2.76 / 1.55~1.60

3.46 m / 2.78 m / 0.67 m

1.42 m / 1.15 m

3.03 -> 7.54 MHz

1.86 -> 5.07 MHz



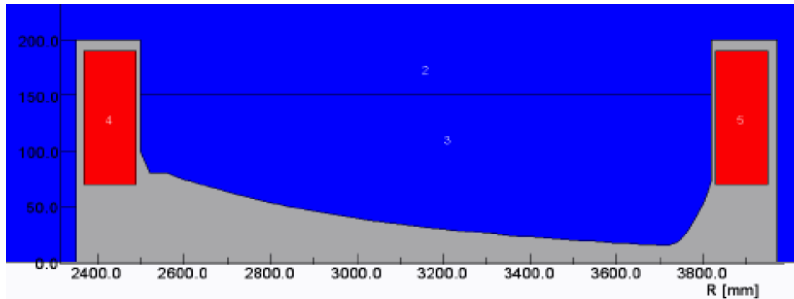
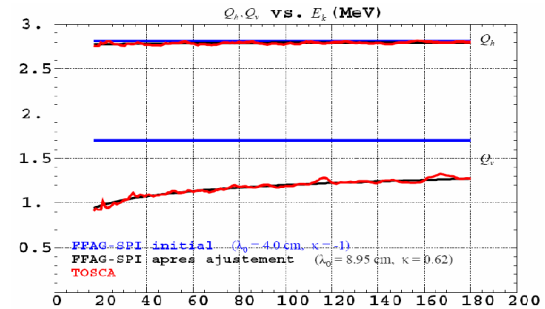
# **MAGNET PROTOTYPING**

## **DESIGN STAGE**

# RACCAM has studied two types of magnets and constructed and tested a prototype

## Issues :

- Need vertical tune constant, whatever the radius
- Good to have a knob for adjusting  $k$

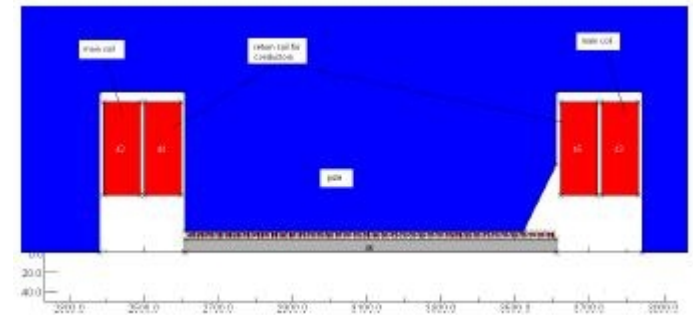


## Gap shaping magnet:

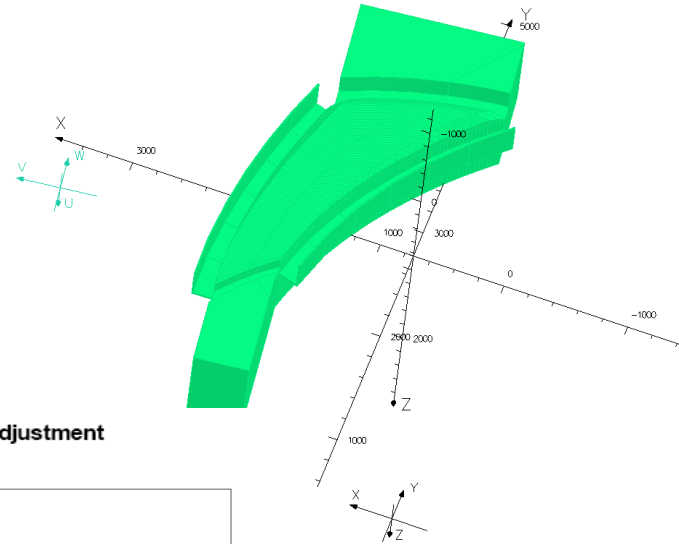
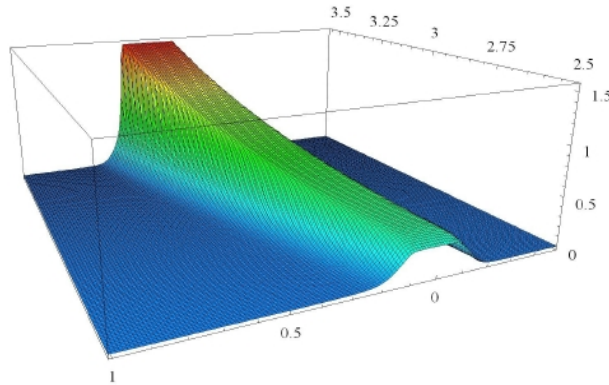
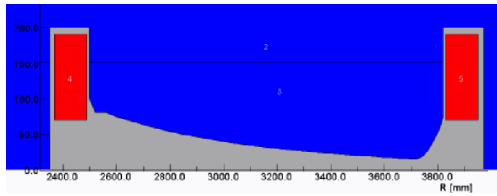
- Less consuming
- Rather straightforward technology
- Selected for prototyping
- Designed, constructed, measured by SigmaPhi

**Parallel gap magnet** with distributed pole conductors that generate the  $B \sim r^k$  law :

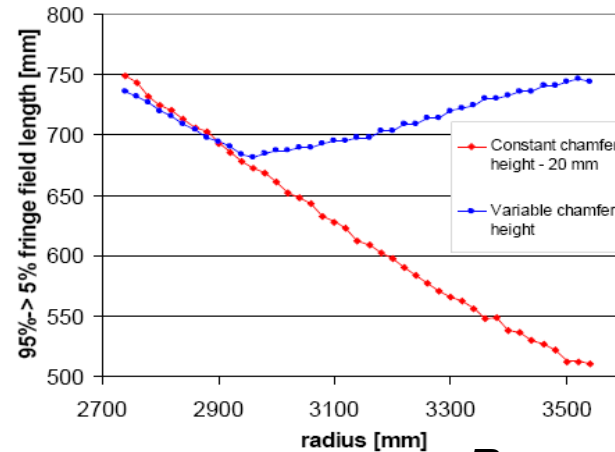
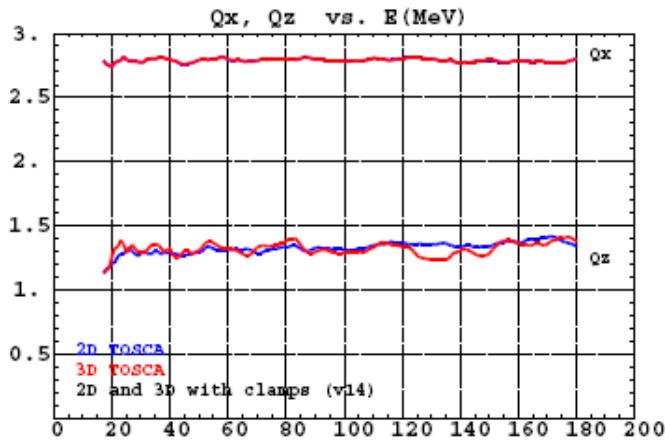
- Would provide knob for  $k$
- Expected to yield lower  $Q_z$  variation with radius
- Design principles studied by SIGMAPHI/InfinitesiMag



• **Gap shaping magnet prototype. The design stage** using TOSCA 2D and 3D, showed that stabilization of vertical tune can be achieved by combination of *variable chamfer* and *field clamp*.



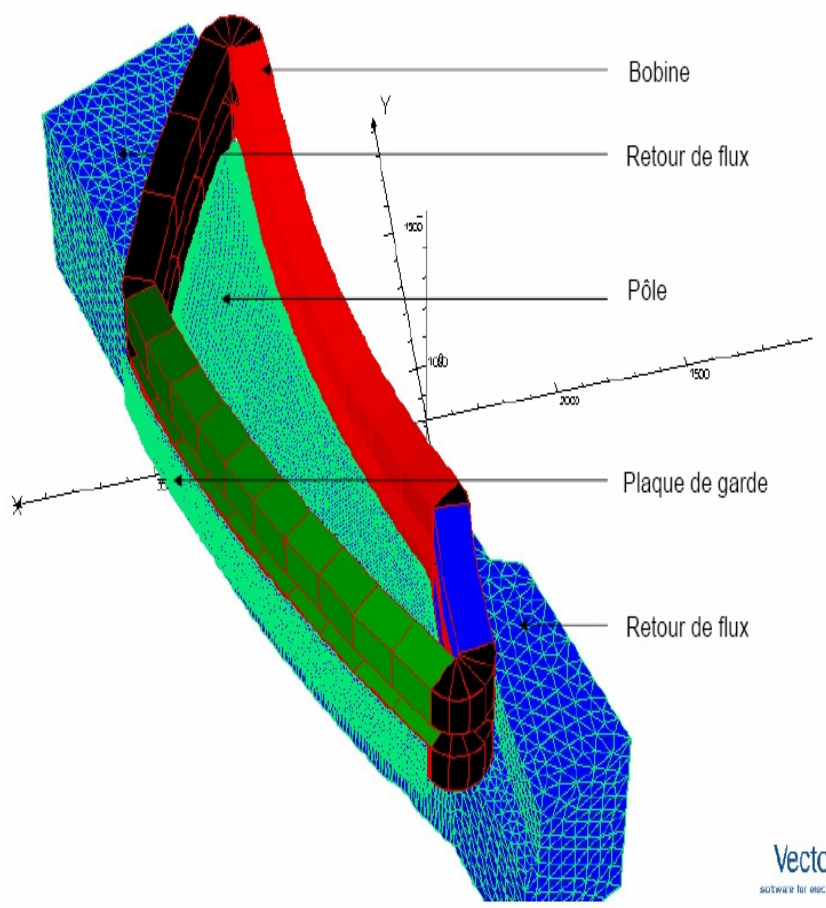
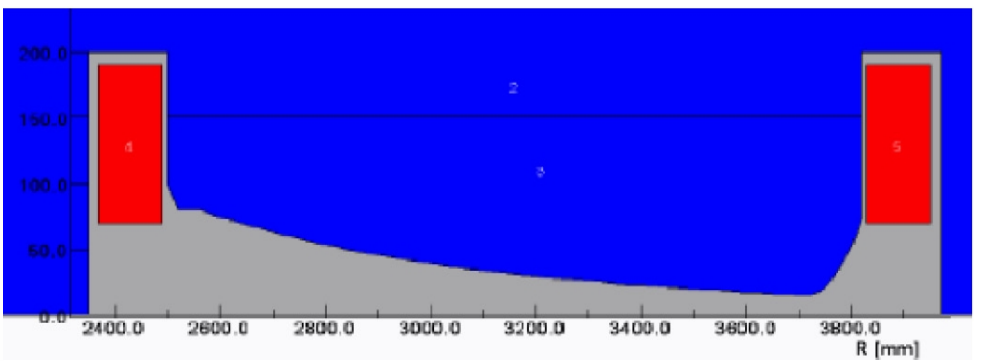
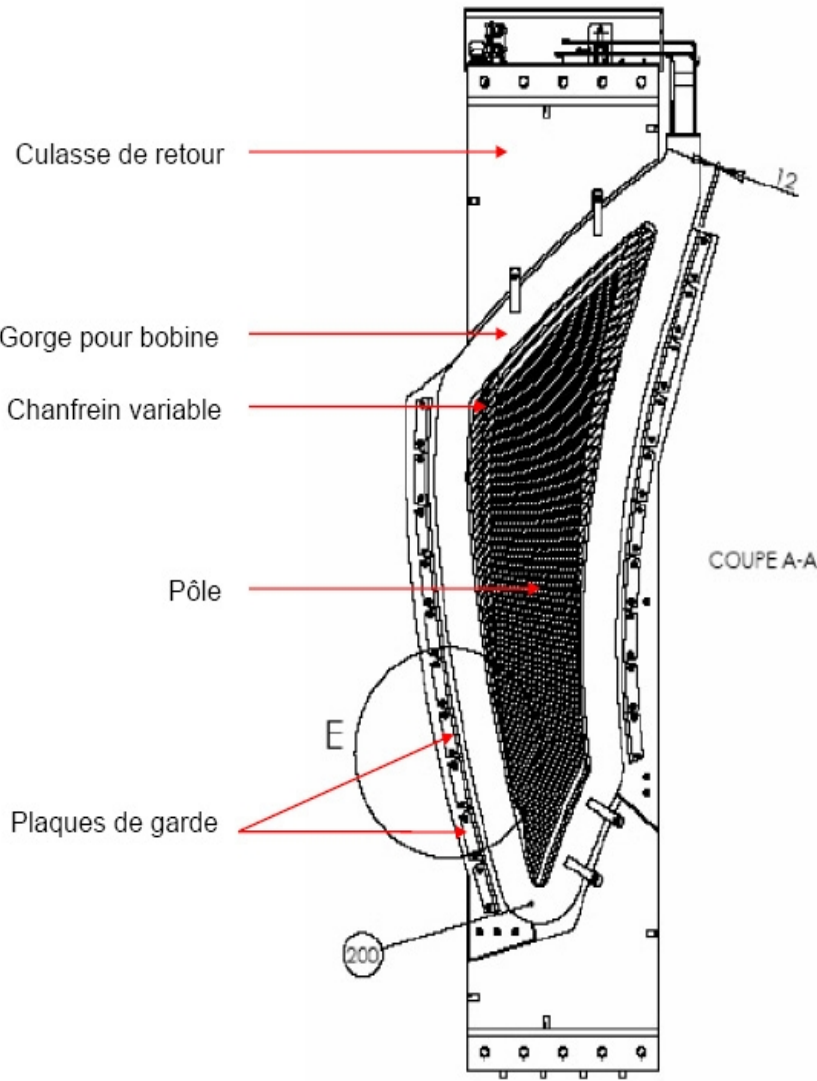
Fringe field length adjustment



Remember :

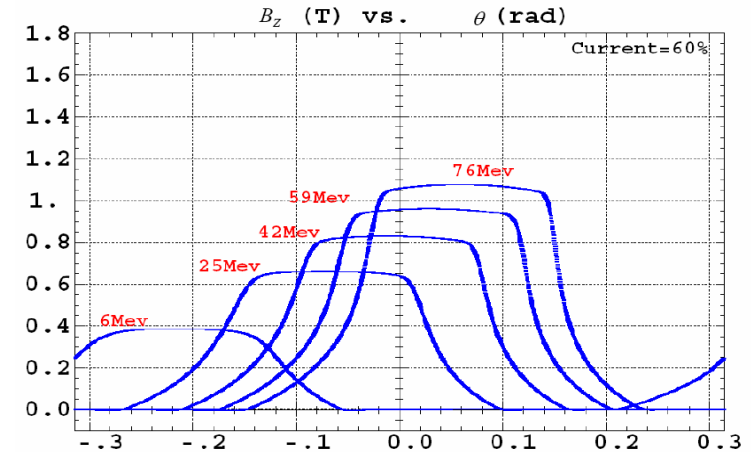
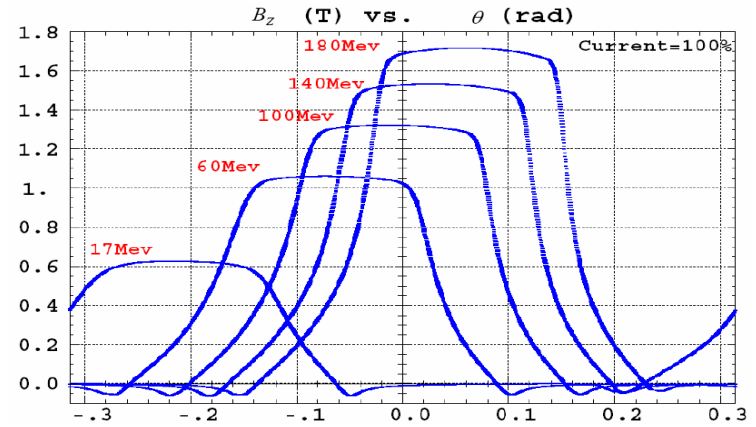
$$\psi = I_1 \frac{\lambda}{\rho} \frac{1 + \sin^2(\delta)}{\cos(\delta)} \quad \text{requires } \lambda \sim r$$

# Sample results from TOSCA modelling

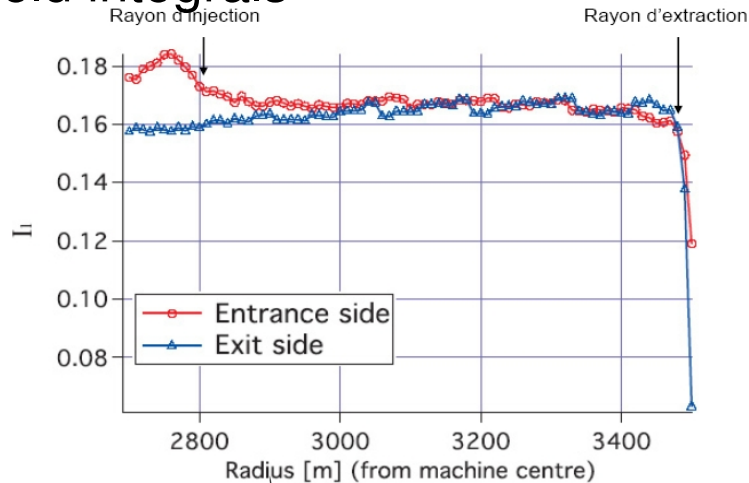


# • Prototype gap shaping magnet : design field on closed orbits

Mode	Energie d'injection / extraction	$B_{z0}$
100%	17 – 180 MeV	1.71 T
90%	13 – 157 MeV	1.59 T
80%	11 – 130 MeV	1.43 T
70%	9 – 102 MeV	1.25 T



## Field integrals



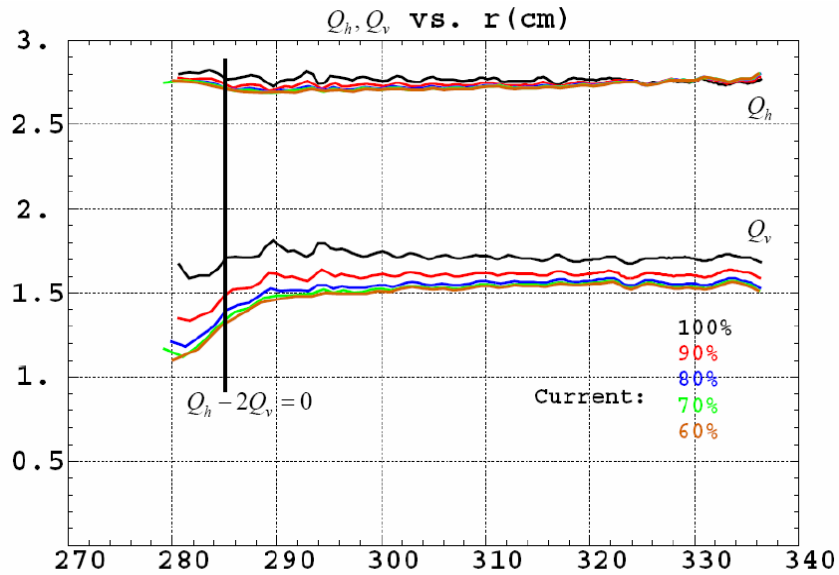
$$M_z = \begin{pmatrix} 1 & 0 & 0 \\ -\frac{\tan(\delta - \psi)}{\rho} & 1 & 0 \\ 0 & 0 & 1 \end{pmatrix} \quad \psi = I_1 \frac{\lambda}{\rho} \frac{1 + \sin^2(\delta)}{\cos(\delta)}$$

$$I_1 = \int_{-\infty}^{\infty} \frac{B_z(s) [B_{z0} - B_z(s)]}{\lambda B_{z0}^2} ds$$

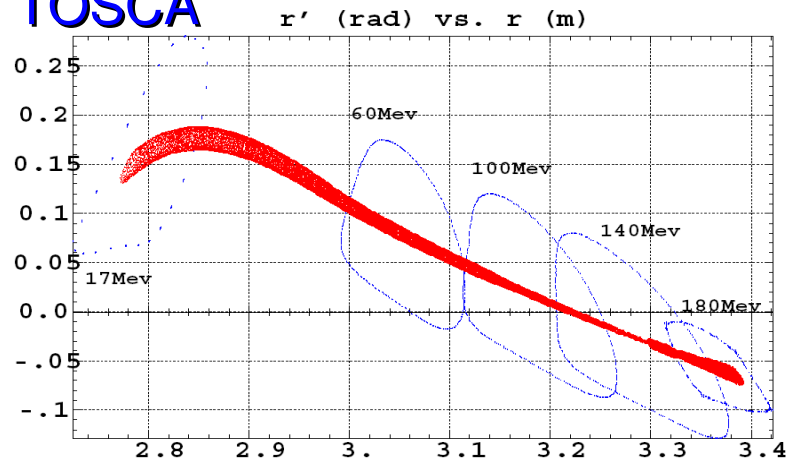
- **Prototype gap shaping magnet,**

design orbits, including,

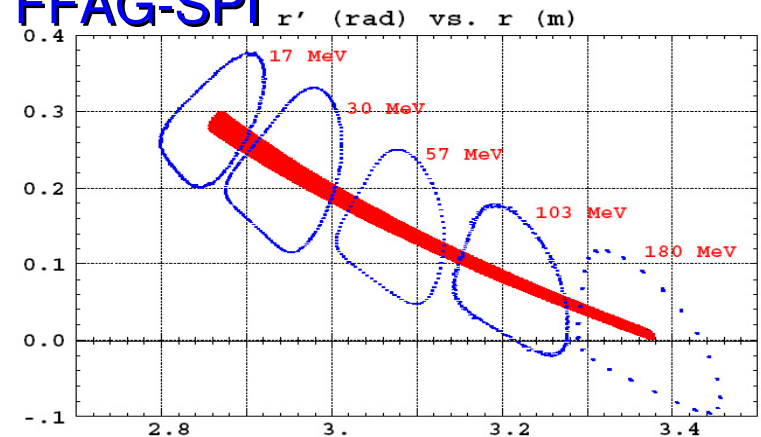
- tune behavior
- horizontal DA
- possible emittance increase upon resonance Xing



## TOSCA



## FFAG-SPI



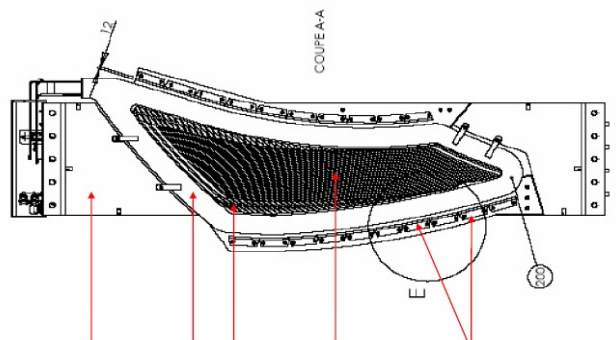
For comparison :  
FFAG-SPI model

# **PROTOTYPE MAGNET : FABRICATION**

yoke shape		paralimpepic
gap shape		laminated
gap at $r_{str}$ ( $g_0$ )	cm	4
gap at $r_{inj}$	cm	~ 11.6
pole extent, $r_{min} - r_{max}$	m	2.61 - 3.61
chamfers		variable
field clamps		spiral
lamination thickness	mm	1.5
overall magnet dimensions, $L \times W \times H$	mm	2913 $\times$ 579 $\times$ 1230
total weight of magnet	t	18
coil		
cross section	mm	113.6x115.6
average winding length	m	5.157
weight	kG	271
resistance, 20 °C	$\Omega$	0.335
voltage	V	79.43
current	A	225
dissipated power, per coil	kW	17.873
number of cooling circuits		6
total water flow	l/min	12.13
water temperature, in / out	°C	25 / 44

to minimize magnet weight  
to allow for  $dB/dt \approx 0.1$  T/s  
Fig. 1,  $g(r) \approx g_0(r/r_0)^{-k}$   
determined by beam size  
determined by gap law  
so to ensure scaling field law  
follow  $r = r_0 e^{\theta/\tan\zeta}$  line ?  
contribute to scaling field

# Mechanical and electrotechnical specifications, according to magnet design



## Values met by the constructor

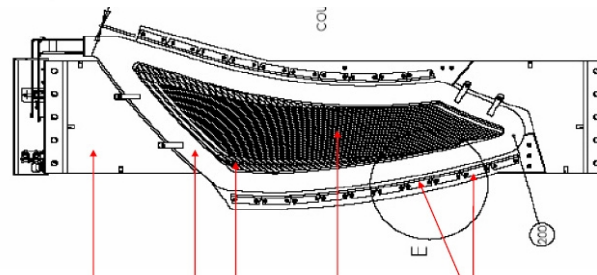
CARACTERISTIQUES ELECTRIQUES (AIMANT) / ELECTRICAL PARAMETERS (MAGNET)	
Courant / Current	225 A
Mode d'alimentation / Supply mode	Autre / Other
Resistance à 20°C / Resistance at 20°C	647.40 m $\Omega$
Tension à chaud / Voltage drop at warm	153.30 V
Electrical power	34.477 KW
Amperes.tour / Amperes.turn	64800 A.t
Inductance	Not calculated
Densité de courant dans le conducteur / Current density in the conductor	A/mm <sup>2</sup>
Autre / Other	
CARACTERISTIQUES THERMIQUES / THERMAL PARAMETERS	
Type de refroidissement / Cooling type	Par eau / Water cooling
Echauffement / Temperature rise	18°C
CARACTERISTIQUES HYDRAULIQUES (AIMANT) / HYDRAULIC PARAMETERS (MAGNET)	
Perte de charge / Pressure drop	4 Bar
Débit / Water flow	24.7 Liter / Minute
Pression de service / Operating pressure	10 Bar
CARACTERISTIQUES MAGNETIQUES / MAGNETIC PARAMETERS	
Champ / Field	1.7T

# Beam related specifications, from magnet design

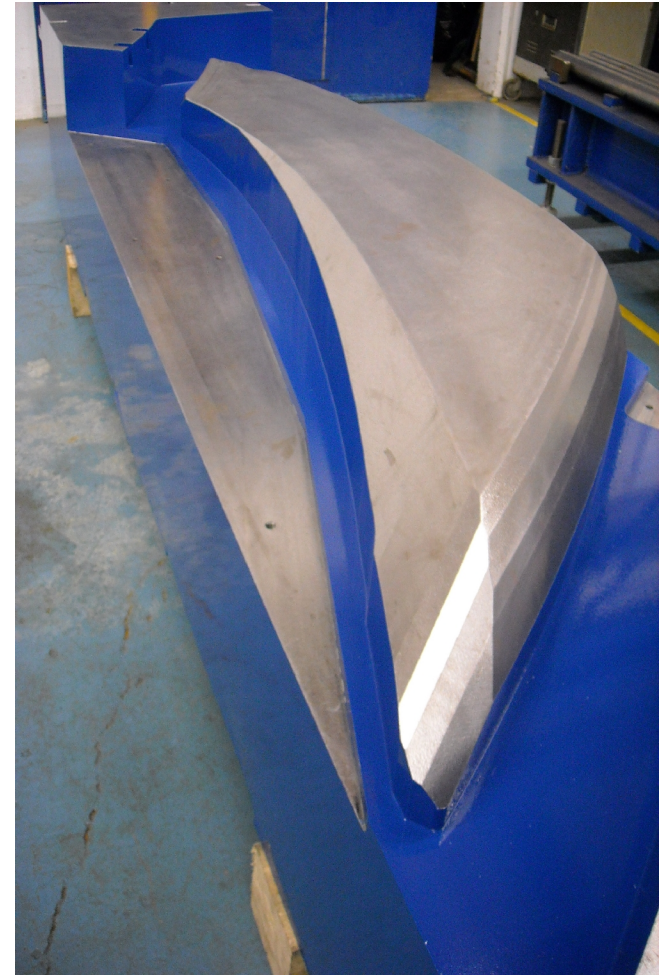
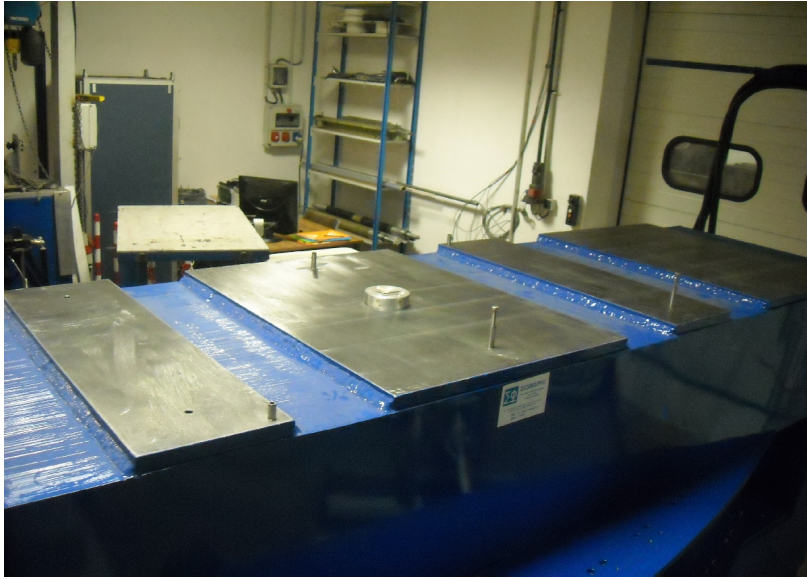
Table 3: Specifications to be met by the RACCAM magnet prototype.

			<i>Comments</i>
magnet shape		spiral	EFB <sup>(*)</sup> defined by $r = r_0 e^{\theta / \tan \zeta}$
field shape		scaling	$B(r) = B_0 B_r(r) B_\theta(r, \theta)$
radial field dependence		scaling	$B_r(r) = (r/r_0)^k$
axial field dependence		spiral	$B_\theta(r, \theta) = \mathcal{F}(r, \theta)$
field index ( $k$ )		5.00	
spiral angle ( $\zeta$ )	deg.	53.7	
sector angle ( $A$ )	deg.	12.24	
bending angle ( $\beta$ )	deg.	36	$2\pi/N$
packing factor		0.34	$\beta/A$
energy range, high	MeV	17 → 180	
energy range, low	MeV	6.3 → 70	
$B\rho_{tr}/B\rho_{inj}$		3.391	
max. radius of GFR <sup>(*)</sup> ( $r_{GFR,max}$ )	m	3.4	$E \approx 150$ MeV
min. radius of GFR <sup>(*)</sup> ( $r_{GFR,min}$ )	m	2.9	$E \approx 25$ MeV
max. field on $r_{GFR,max}$	T	1.5576	
max. field on $r_{GFR,min}$	T	0.7032	
fringe field extent ( $\lambda$ )	m	prop. $r$ ?	$\lambda(r)$
$I_1$ integral		1/6	
horizontal good field region	m	2.9 – 3.4	$E : 20 \rightarrow 150$ MeV
orbit excursion	m	0.5	
vertical good field region	m	$\approx \text{gap}/2$	
horizontal tune $\nu_x$		2.76	
vertical tune $\nu_z$		1.56 – 1.59	
dB/dt	T/s	0.3	stabilized in less than 100 ms

(\*) Good field region



- The magnet has been built by SIGMAPHI



# **PROTOTYPE MAGNET : MAGNETIC FIELD MEASUREMENTS**

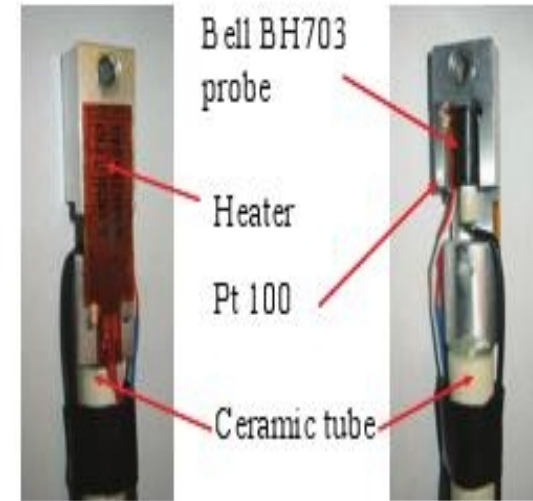
# • Magnetic measurements

## MEASUREMENT SYSTEM AND ACCURACY



MAPPING system

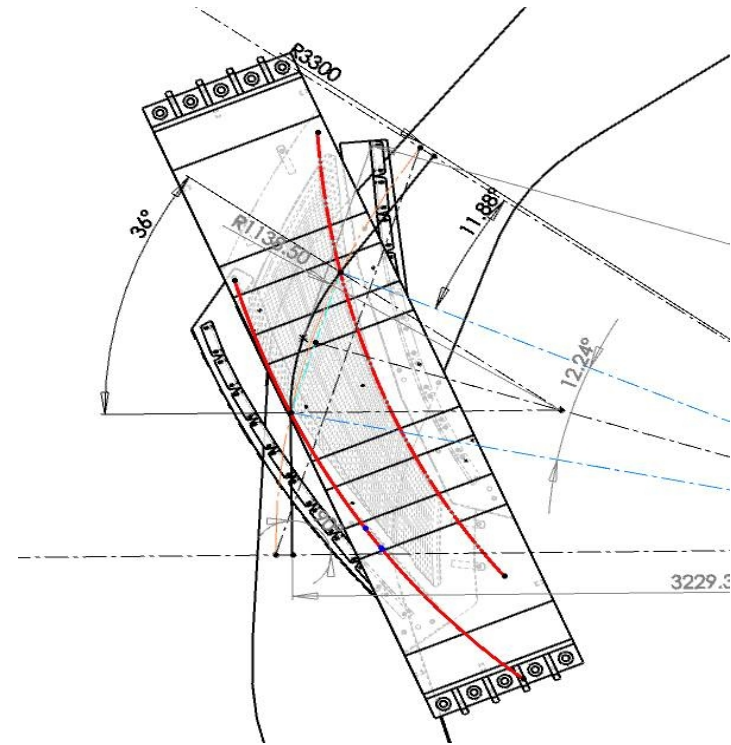
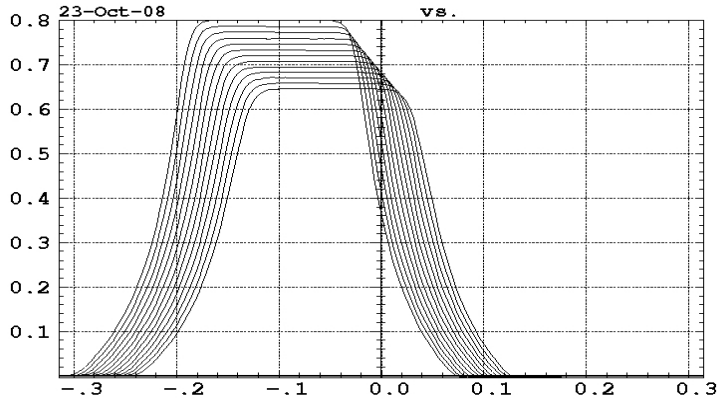
- 3 axis Hall probe Bell BH703, temperature regulated  $30^{\circ}\text{C} \pm 0.1^{\circ}\text{C}$
- Air-conditioned laboratory ( $20^{\circ}\text{C} \pm 1^{\circ}\text{C}$ )
- Field acquire in 3D with a 20 channels multimeter
- Automated Mapping table  $1600 \times 600 \times 300$
- Hall probe calibration until 1.8T, accuracy  $3 \cdot 10^{-5}$
- Current stability  $< 5 \cdot 10^{-5}$
- Hall tension stability  $< 0.2$  Gauss



3 AXIS HALL PROBE



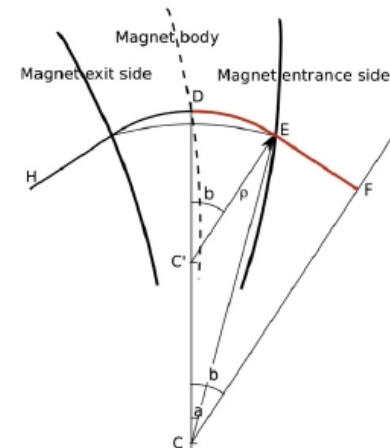
# • Magnetic measurements



The bulk of the measurements : field on 11 arcs around given R :  
 $R=2750, 2900, 3125, 3300, 3450\text{mm}, \pm 55\text{mm}, \text{step } 11\text{mm}.$

Done for current in coil of

- 225 Amp** → 1.93 T at 3.46 m (227 MeV)
- 80%** → 1.61 T (162 MeV)
- 60%** → 1.23 T (98 MeV)



product number RACCAM  
magnet number proto  
date and time 16:05 Oct. 20 2008  
operator BD MJL  
power supply Teckelec  
current 134.54  
calibration sept 2008  
alignment 1  
plane 0

# • Magnetic measurements

Typical result data sheet, at given range  $R_i \pm 55\text{mm}$

Bo ref (T) -0.000202  
lo ref (A) 134.5424  
  
dBo' (Gauss) 0.169053821846605  
dlo' (mA) 2.45292000005293

trajectory number 1  
radius (mm) 3125

average current (A) 134.542235299468  
dl/I 3.548533E-05  
Bo' (T) -0.000200247120160589  
lo' (A) 134.544428895  
BL (T.mm) 505.885212406895  
Leff (mm) -802992.400645865  
BL' (T.mm) 505.892841139384  
Leff' (mm) -803004.509745054

I(A) S (mm)  
134.54279601  
134.54318139  
134.543874225  
134.543386845  
134.5425936  
134.54265273  
134.54396997  
134.5436901  
134.54213934  
134.542668135  
134.54307276  
134.54286615  
134.54313933  
134.54336622  
134.542886145  
134.541251925  
134.541315855  
134.54202519  
134.542559085  
134.542708455  
134.543050815  
134.54266305  
134.54110908  
134.54265918

Bx' (T)  
0 -4.40555886854806E-06  
-6.71516828434976E-06  
-1.5083741228815E-05  
-2.31711875462776E-05  
-3.66599568322746E-05  
-5.41474621126063E-05  
-8.11101358072387E-05  
-0.000119002478299474  
-0.000180007120272256  
-0.000288781087814502  
-0.000489362703287365  
-0.000886865983967809  
-0.00171134879284399  
-0.00312856876128646  
-0.00474535988718232  
-0.00584485101822694  
-0.00640055964991634  
-0.00666163887333702  
-0.00678134961692702  
-0.00683175801275004  
-0.0068268832403686  
-0.00682403652947264  
-0.00678678420120075  
-0.00676963856803778

By' (T)  
-0.00020178076496973  
-0.000173860930283967  
-0.00014450812779144  
-0.000110181750828479  
-6.44735929806508E-05  
-1.11150090658309E-05  
6.16329994040072E-05  
0.000153409929871422  
0.000283658936709981  
0.000470136526019504  
0.000747077905775863  
0.00124443548650822  
0.00225260648318265  
0.00443311405817762  
0.00844660434350137  
0.0141376656356812  
0.0208894717430771  
0.0284339396929519  
0.0365558843055311  
0.0453150813202366  
0.0545747904389083  
0.0644727521440337  
0.0749895849925962  
0.0860332982175262

Bz' (T)  
-5.13163278608349E-06  
-2.81547410028881E-06  
1.825869774473E-06  
1.04986204858515E-05  
1.64599055918868E-05  
2.91068921850812E-05  
4.35289268704956E-05  
7.49343162681751E-05  
0.000115037695365823  
0.000184966572401949  
0.000312082102654512  
0.000572616925150128  
0.00108023746889217  
0.00197751956588934  
0.00309922279276627  
0.00398318418995119  
0.00449966269162818  
0.00478987689528881  
0.00497910690572788  
0.00511415619153322  
0.00522319262827881  
0.00533216276476242  
0.00542258744061969  
0.00552160827087861

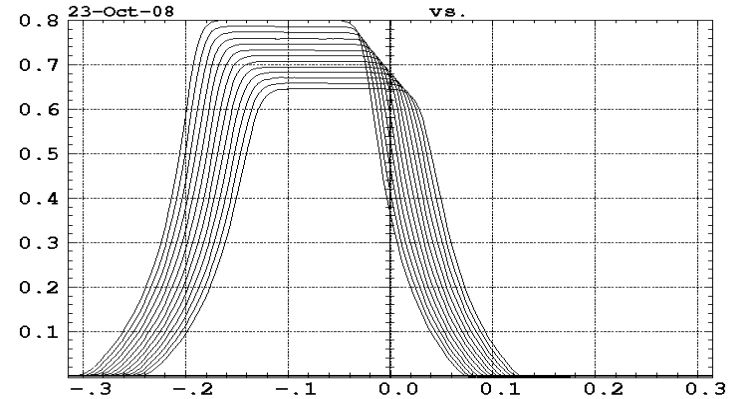
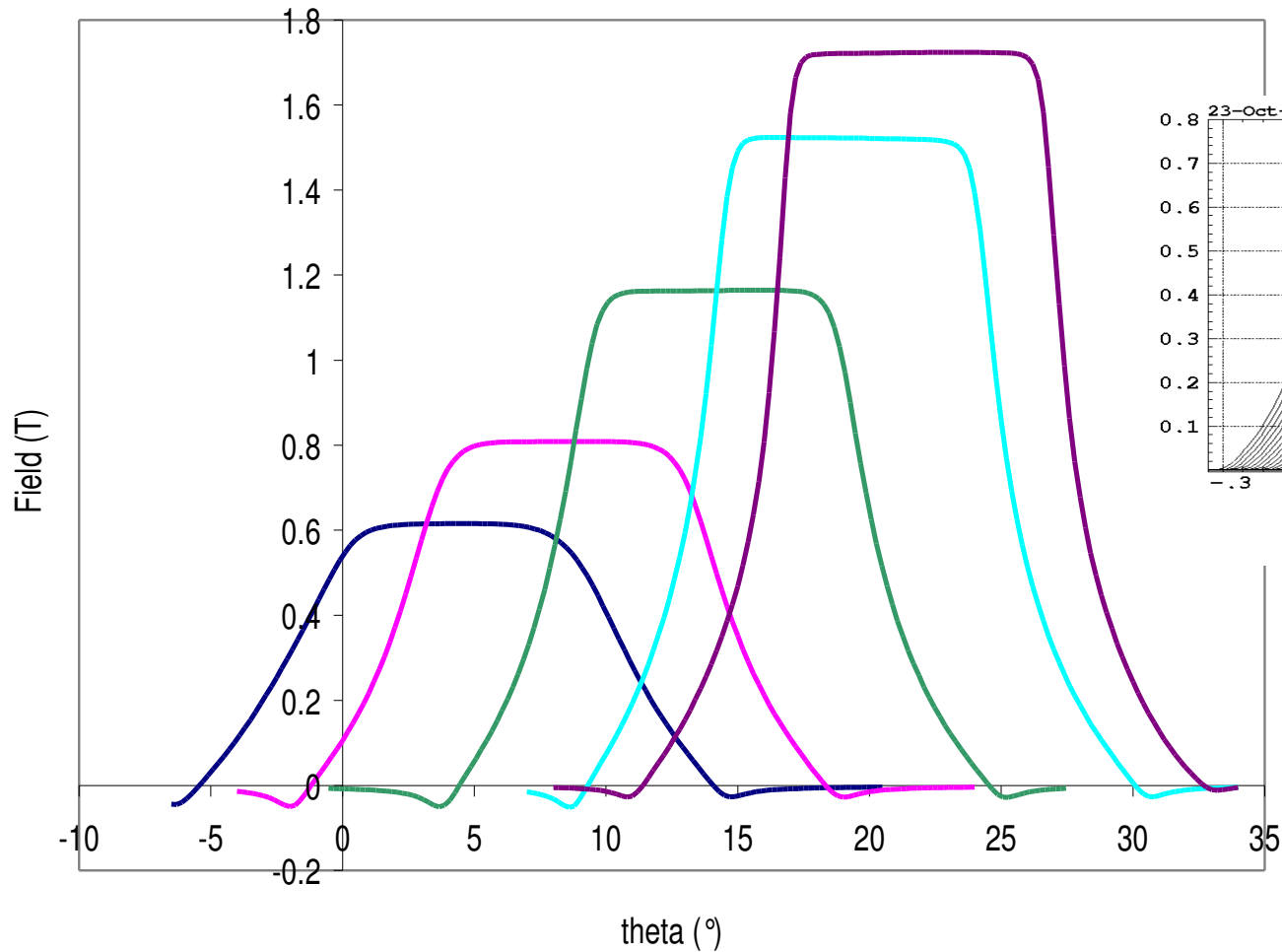
trajectory number  
radius (mm)  
  
average current (A)  
dl/I  
Bo' (T)  
lo' (A)  
BL (T.mm)  
Leff (mm)  
BL' (T.mm)  
Leff' (mm)

I(A)  
134.542194045  
134.54203248  
134.54362353  
134.54197182  
134.541337335  
134.54243883  
134.542343775  
134.542178835  
134.54230155  
134.54184606  
134.5422003  
134.541751725  
134.542336245  
134.54217753  
134.542081635  
134.542037595  
134.54317419  
134.541902205  
134.54235837  
134.542520895  
134.542789275  
134.541978405  
134.542201725  
134.54236056

# • Magnetic measurements

Typical result data sheet, at given range  $R_i \pm 55\text{mm}$

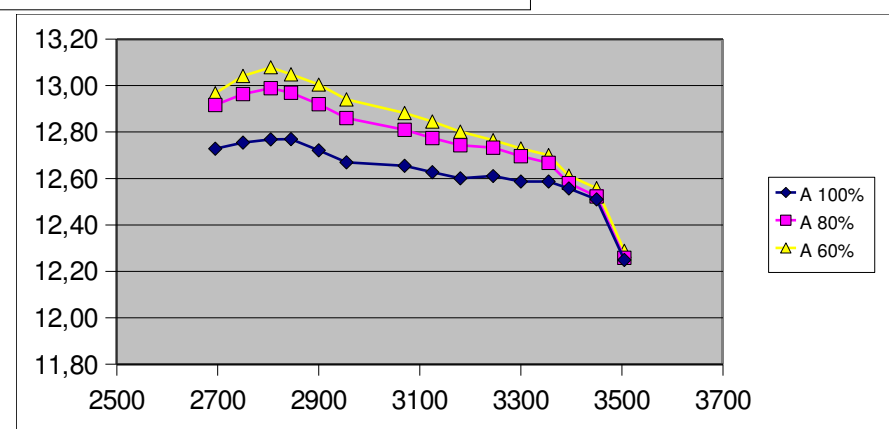
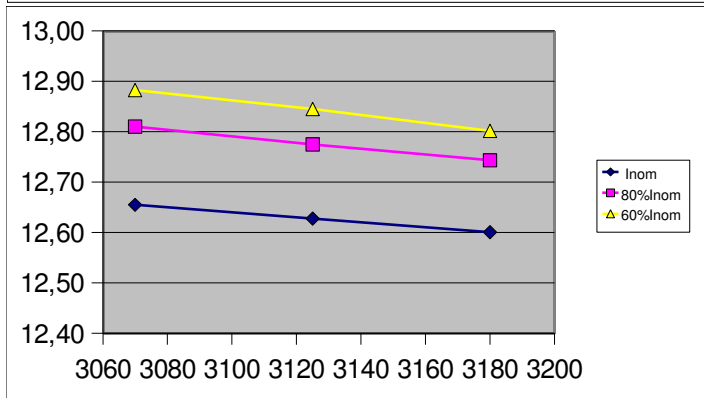
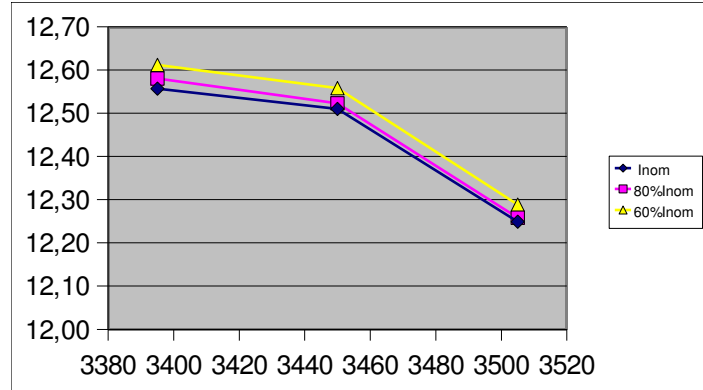
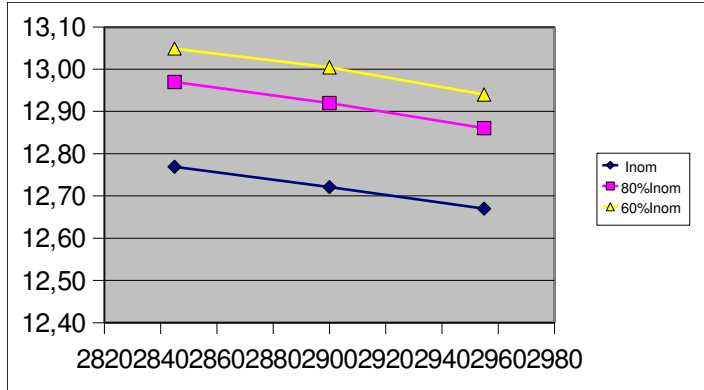
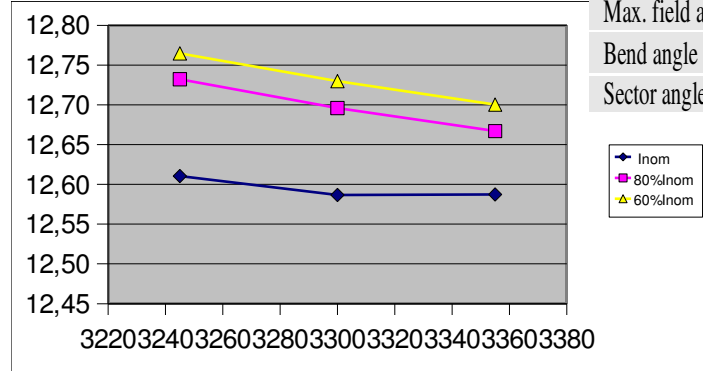
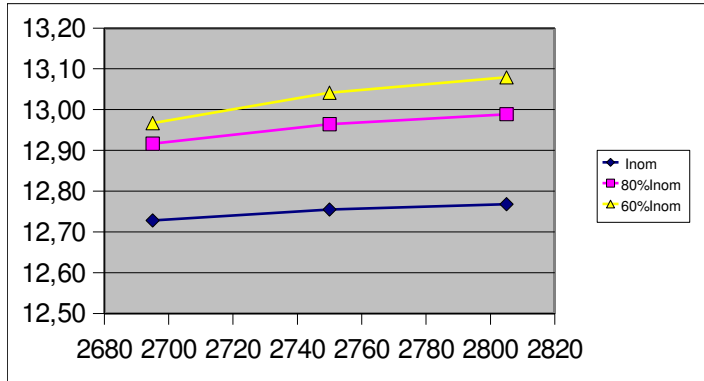
Field versus theta at Inom



# • Magnetic measurements

Sector angle,  $A$ . Theoretical : 12.24 deg

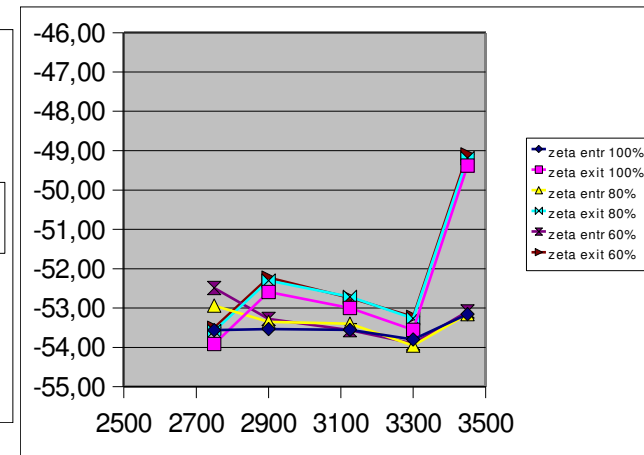
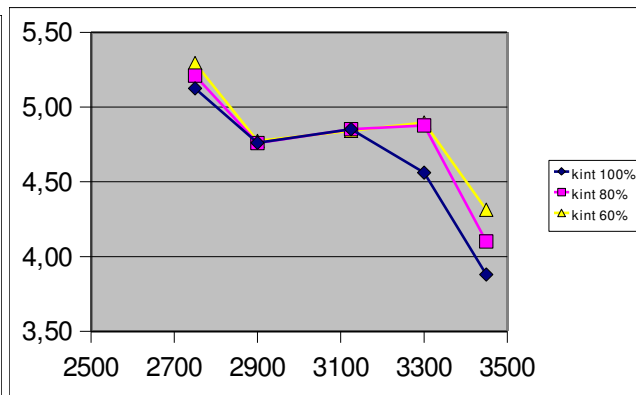
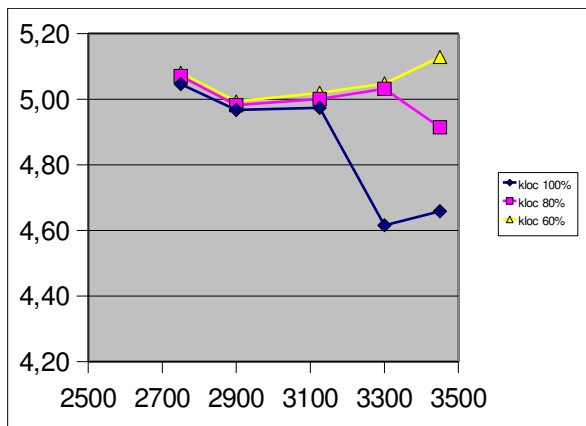
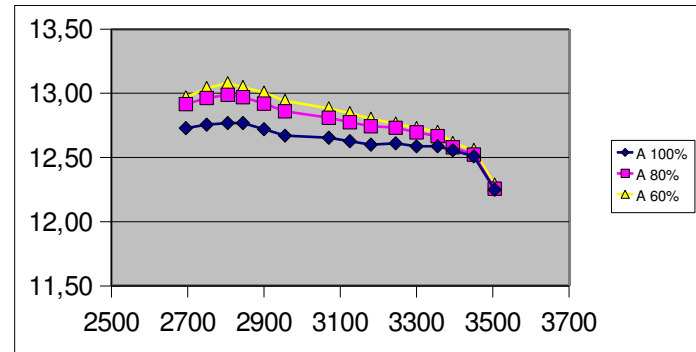
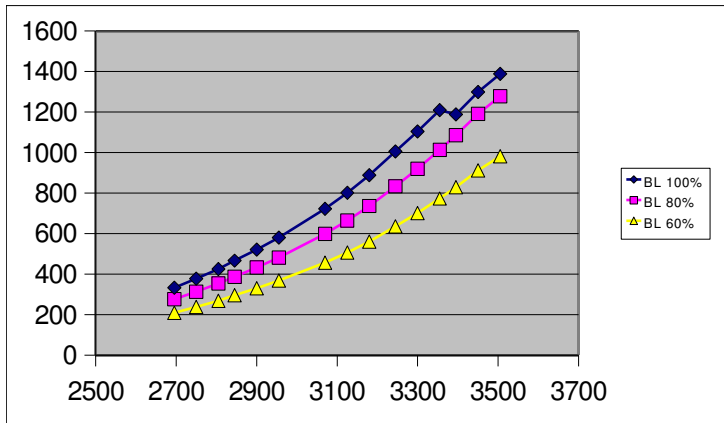
Type	Gap shaping
Packing factor (pf)	0.34
Field index (k)	5
Spiral Angle ( $\zeta$ ) (deg)	53.7
Min./Max. radius of good field region (m)	2.9/3.3
Max. field at min./max. radius (T)	0.58/1.7
Bend angle ( $\beta$ ) (deg)	36
Sector angle ( $A$ ) (deg)	12.24



# • Magnetic measurements

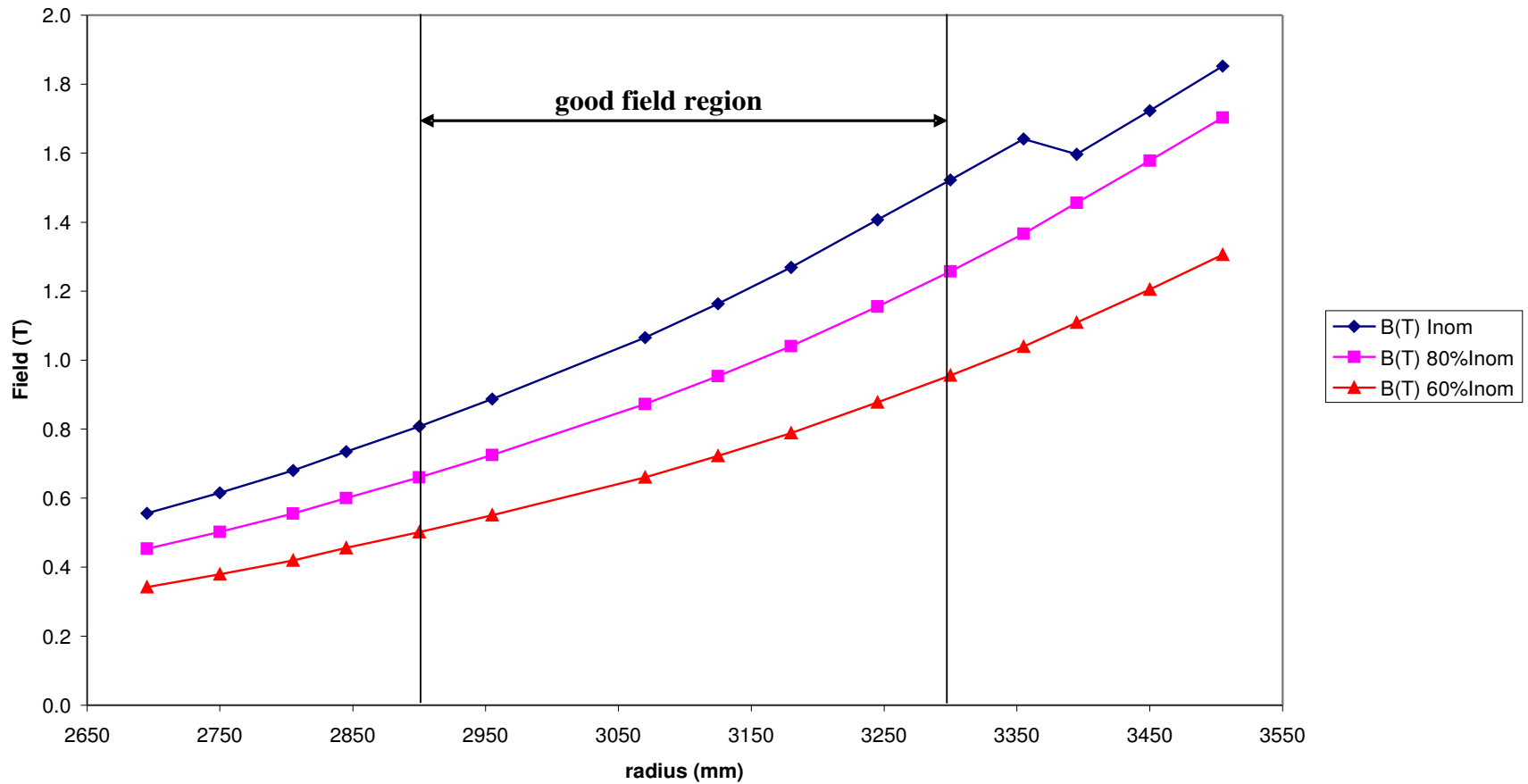
Synthesis : field integrals (th. 36deg, normalized), sector angle A (th. 12.24 deg) local k from B (taken at A/2), average k from BL (th. 5.00), spiral angle at entrance/exit

Packing factor (pf)	0.34
Field index (k)	5
Spiral Angle ( $\zeta$ ) (deg)	53.7
Min./Max. radius of good field region (m)	2.9/3.3
Max. field at min./max. radius (T)	0.58/1.7
Bend angle ( $\beta$ ) (deg)	36
Sector angle (A) (deg)	12.24



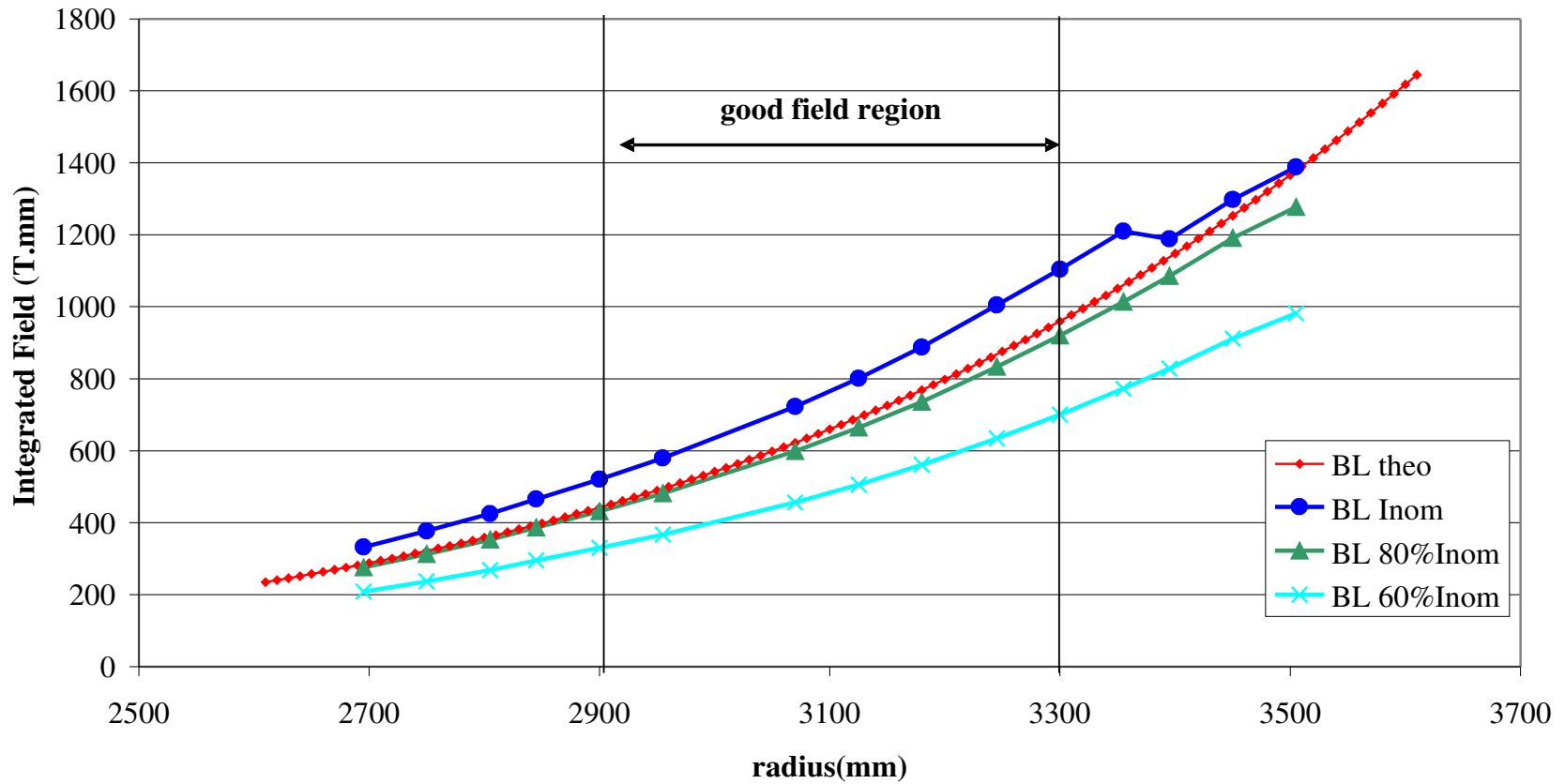
# • Magnetic measurements

Field versus radius at  $\theta = \theta_{mc}$



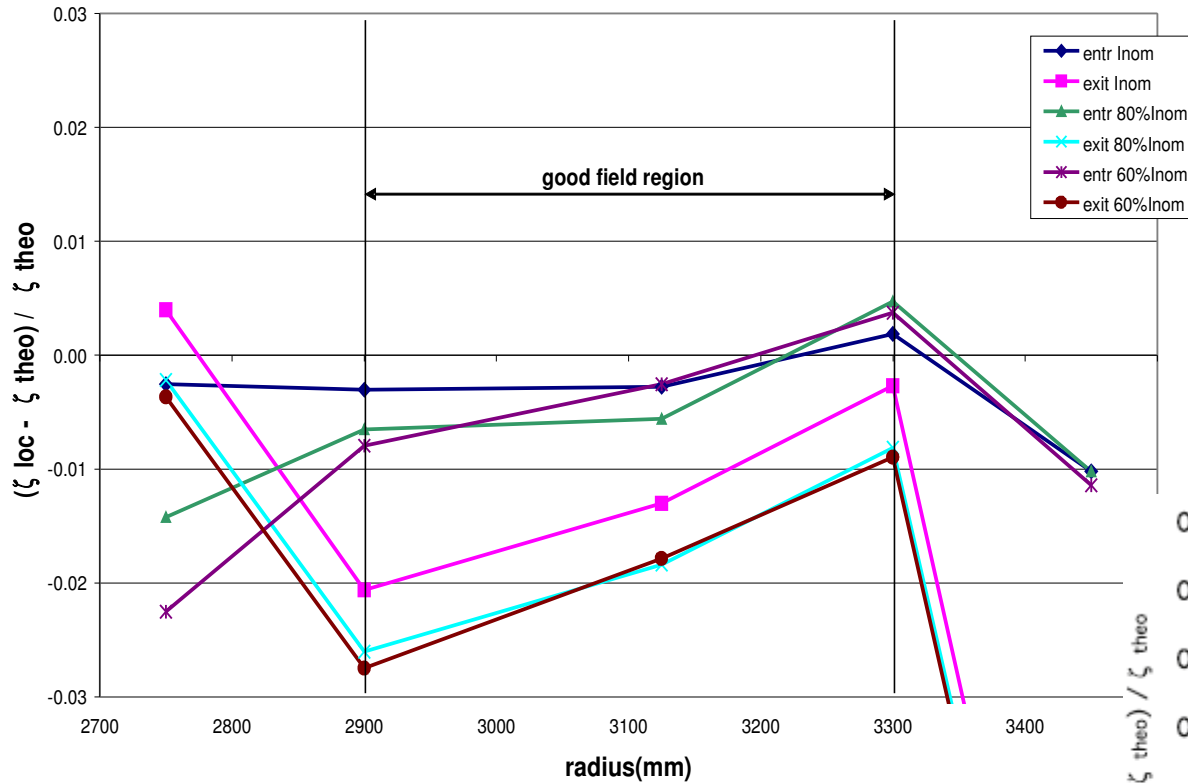
# • Magnetic measurements

**Integrated field versus radius**  
**Comparison between theoretical and measured values**

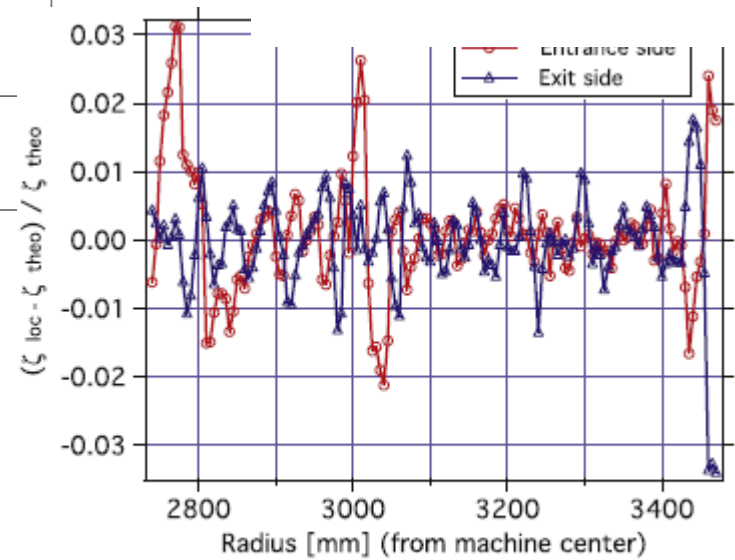
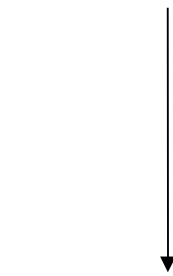


# • Magnetic measurements

Relative error on local value of  $\zeta$ , as a function of radius



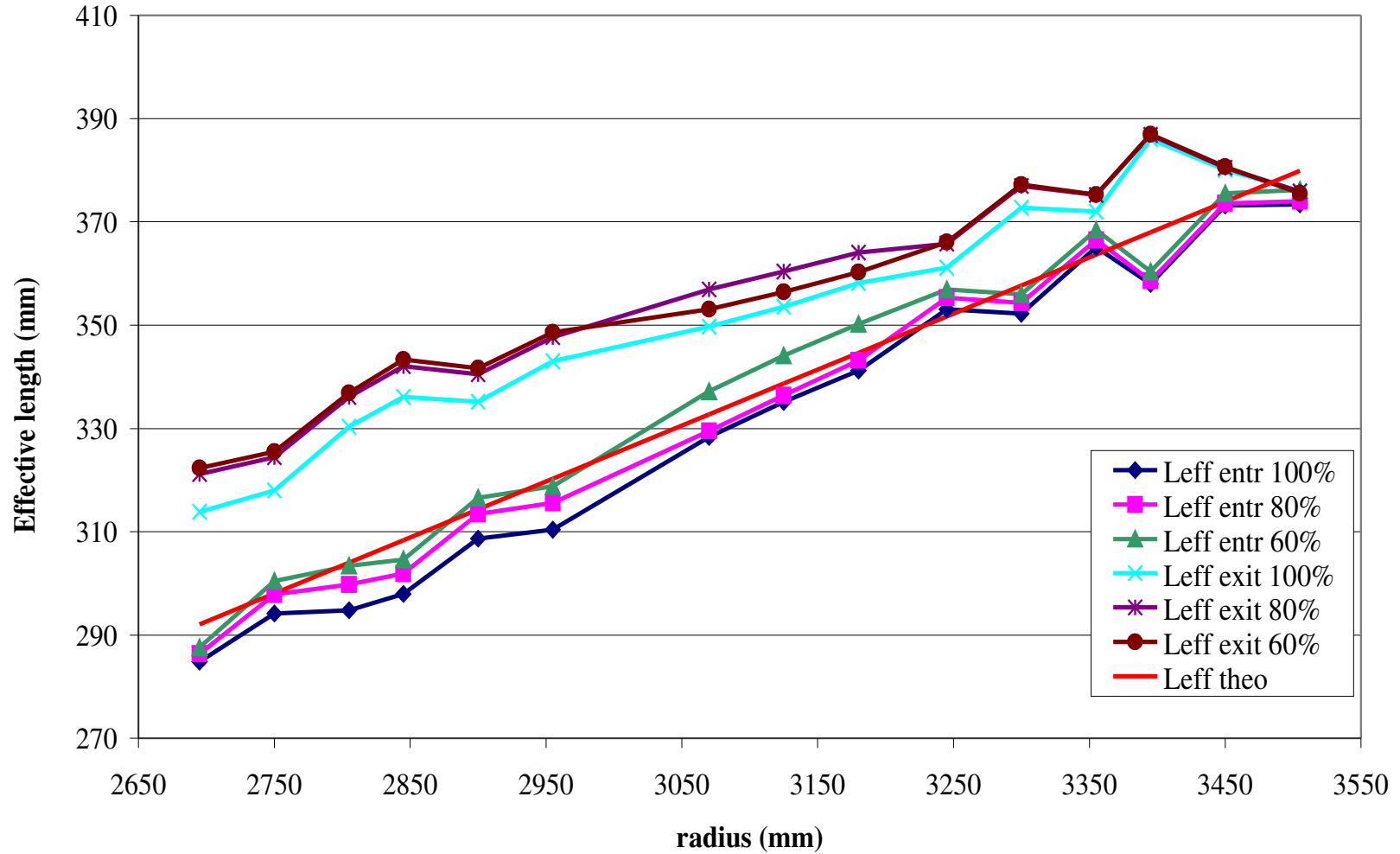
Comparison with TOSCA results



Relative error on local value of  $\zeta$ , as a function of radius.

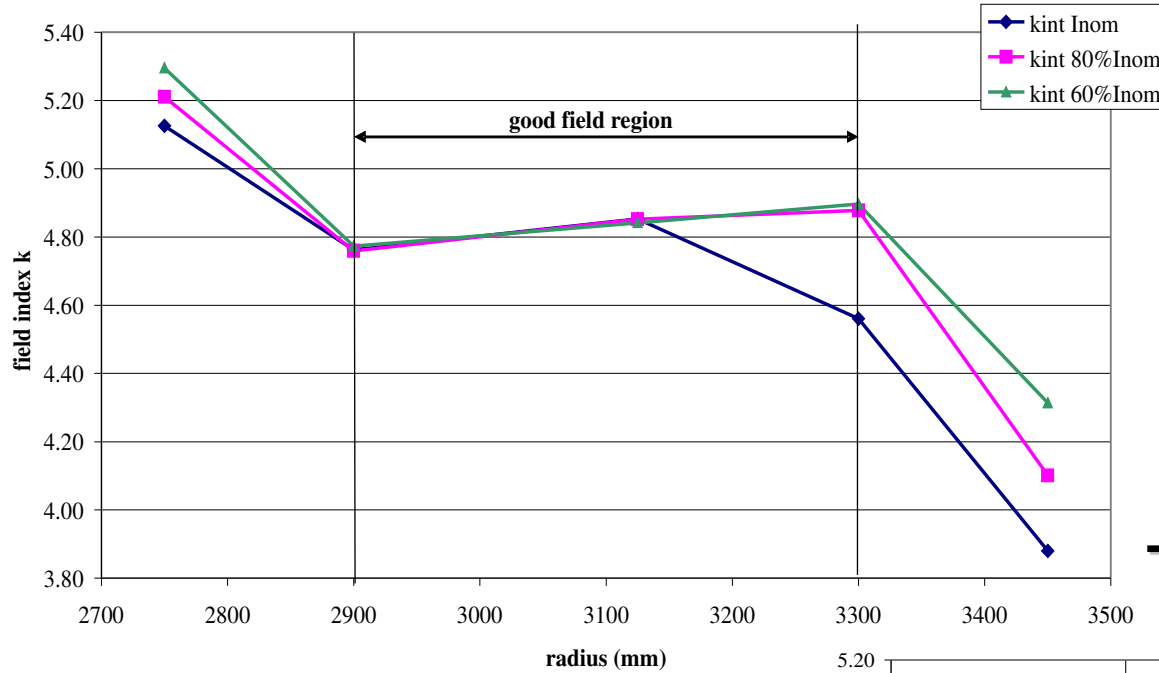
# • Magnetic measurements

Effective length versus radius  
Comparison between theoretical and measured values



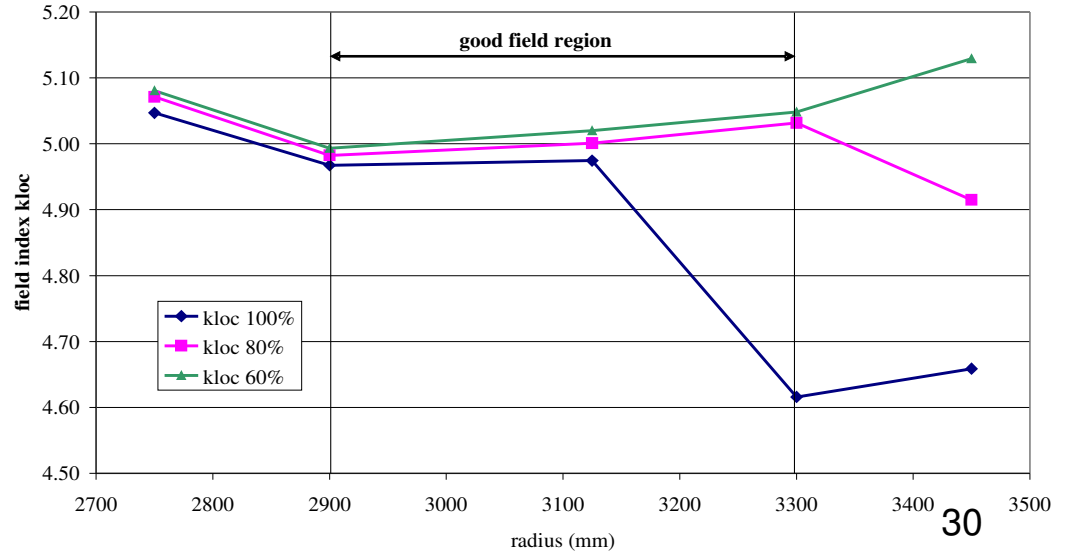
# • Magnetic measurements

Field index (k integrated) versus radius



**Theoretical :  $k=5.00$**

Field index (k local) versus radius



- Prototype gap shaping magnet : tracking in the measured field maps, Zero-th order (3/5) → see PAC 09 Proceedings

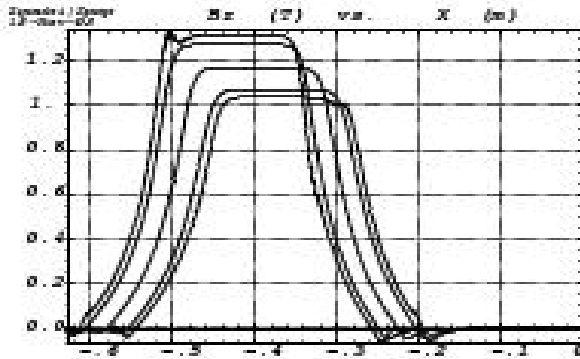


Figure 3: Magnetic field along 5 arcs of circles.

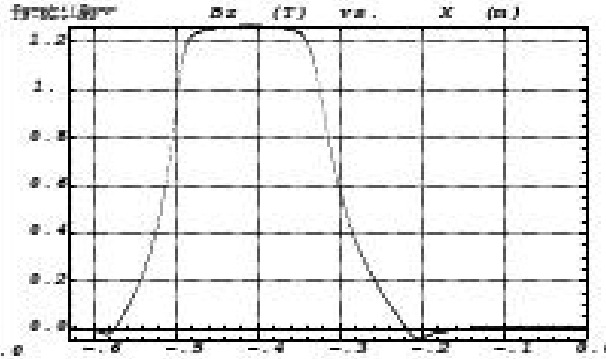


Figure 4: Field on closed orbit in the  $R = 3125$  mm region.

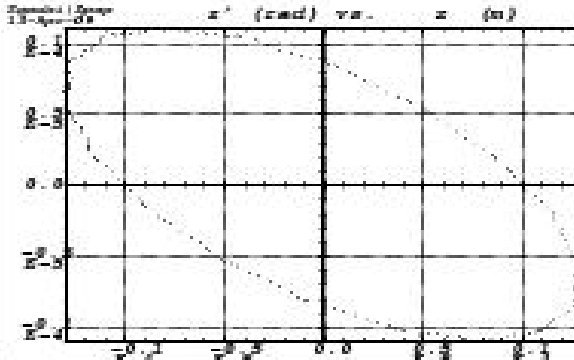
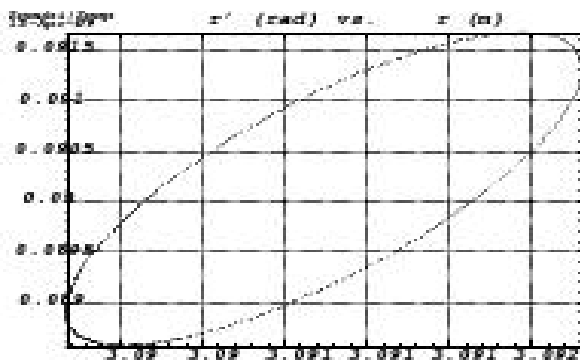


Figure 5: Typical paraxial motion used for tune computation, horizontal (left), vertical (right).

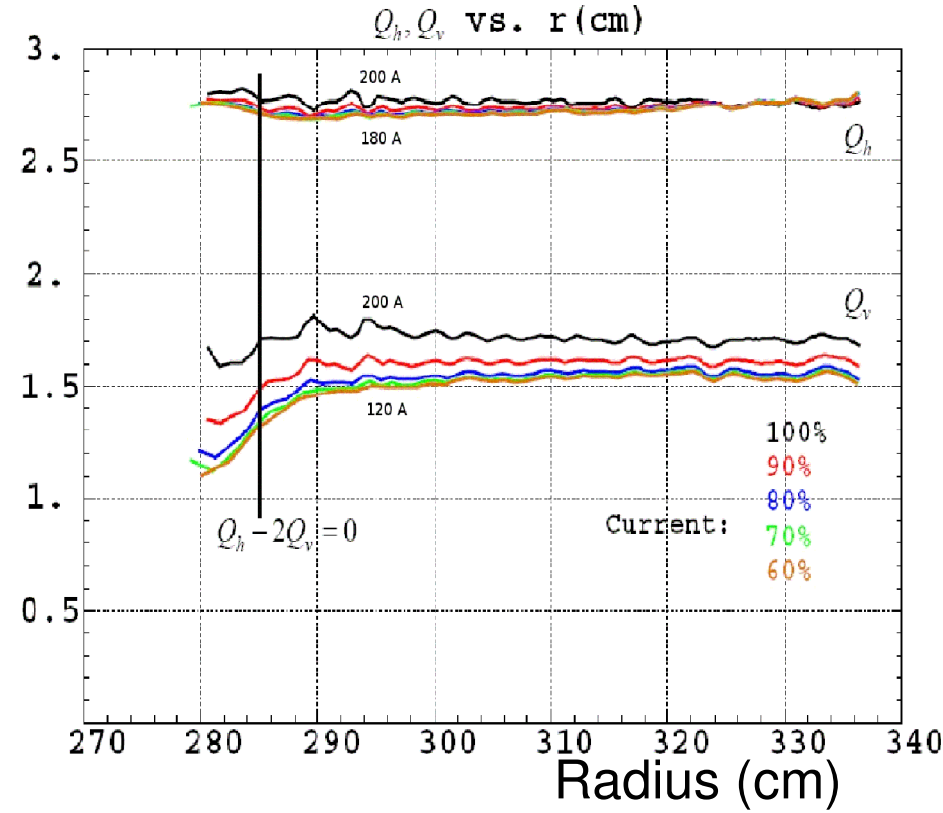
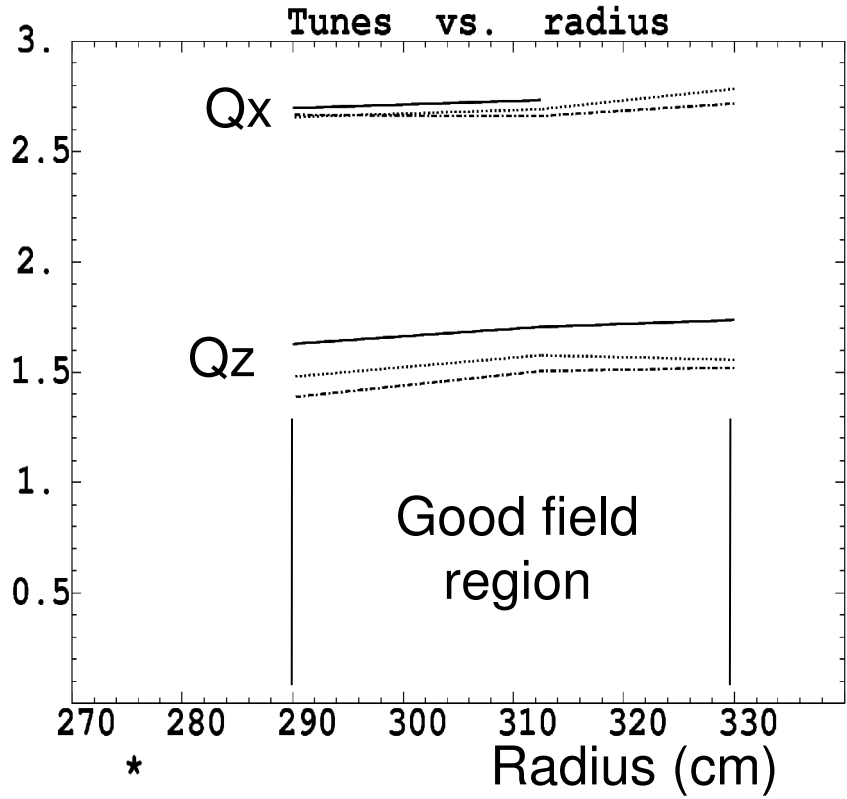
Zero-th order :

$R$ (mm)	$E_{c.o.}$ (MeV)	$\hat{r}$ (mm)	$\hat{B}$ (T)
<i>Maximal current</i>			
2900	38.0	2950	0.880
3125	86.5	3175	1.259
3300	156.0	3350	1.631
<i>80%<math>I_{max}</math></i>			
2900	26.2	2950	0.719
3125	60.8	3175	1.032
3300	112.7	3350	1.356
<i>60%<math>I_{max}</math></i>			
2900	15	2950	0.546
3125	35.9	3175	0.782
3300	67.3	3350	1.031

- Correlation between  $E$  and  $r$  agrees with theory within a few per-mil

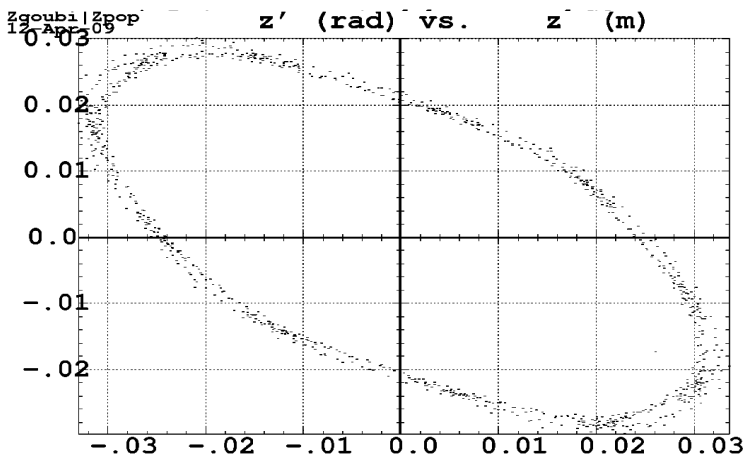
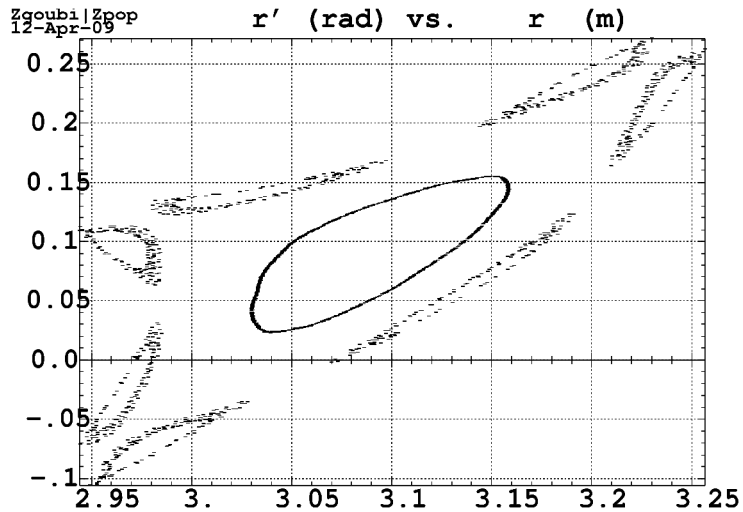
• **Prototype gap shaping magnet : tracking in magnetic field maps, First order (4/5)**

- Tunes, from magnetic measurements (left) and from design simulations using TOSCA (right)



<X>. Sig X. X min. max : 308.4

• **Prototype gap shaping magnet : tracking in magnetic field maps, Dynamic acceptance (5/5) → see PAC 09 Proceedings**



\* Data generated by searchCO

Min-max. Hor. : -3.30113E-02, 3.36319E-02;  
Part# 1-40000 (\*); Limit# 1; pass#

- Large DA's are obtained, consistent with design specifications

Table 4: Dynamic apertures.

<i>R</i> region (mm)	E (MeV)	From measured field maps		From OPERA 3D field maps	
		Ax	Az	Ax	Az
<i>Maximal current</i>		$(B_0 = 1.933 T)$		$(B_0 = 1.7 T)$	
2900	38.0	1800	900	2500	900
3125	86.5	2600	800	2900	1000
3300	156	5500	1500	3500	950
80% $I_{max}$		$(B_0 = 1.606 T)$			
2900	15	4000	1500		
3125	35.9	1500	1200		
3300	67.3	1700	1400		
60% $I_{max}$		$(B_0 = 1.227 T)$			
2900	15	1200	900		
3125	35.9	1200	900		
3300	67.3	2200	900		

# CONCLUSION

**A lot can still be done using measurement data :**

- *Difference with TOSCA simulated field, including*
  - Best fit of mutual relative positioning
  - With possible benefits as,
    - removing the r-dependence of  $L_{eff}$  ? slide 29
- *In general, analyse these data in detail, including*
  - Systematic comparisons with TOSCA simulations
  - Understanding effects as
    - The local value of  $k$ , the integral value of  $k$
    - The offset in the spiral angle
- *The magnet is still there, it can be thought of experimenting further :*
  - Moving the clamps
  - Presence of magnetic (RF) material in the drift region
  - Response to  $dB/dt$
  - etc...

# THANK YOU FOR YOUR ATTENTION

